Journal of Constructional Steel Research 237 (2026) 110076

Contents lists available at ScienceDirect

Journal of Constructional Steel Research

journal homepage: www.elsevier.com/locate/jcsr

# Fire performance of single-storey steel structures - case study: Industrial hall and retail building

Batuhan Der [a,*], Oriana Ilnica [a], Nicola Tondini [a], Thomas Gernay [b], Antoine Glorieux [c]

[a] Department of Civil, Environmental and Mechanical Engineering, University of Trento, Via Mesiano 77, 38123 Trento, Italy
[b] Department of Civil and Systems Engineering, Johns Hopkins University, Baltimore, MD 21218, USA
[c] ArcelorMittal Global Research and Development, 66, Rue du Luxembourg, L-4009 Esch-sur-Alzette, Luxembourg

ARTICLE INFO

*Keywords:*
Fire design
Prescriptive
Performance-based
Localised fire
Case study
Protection

ABSTRACT

Steel structures must be designed for adequate performance in case of fire. This study aims to compare fire design methodologies for portal frame structures based on a prescriptive approach against a performance-based approach relying on the natural fire models recently incorporated into the Eurocodes. The focus is on portal frame structures representative of industrial halls and retail buildings, which are characterized by large open spaces where flashover is unlikely to occur. The prescriptive design approach assesses structural response under the ISO 834 standard fire curve, which does not represent a real fire in these large open-plan spaces. Conversely, the performance-based design approach incorporates natural fire models developed to reflect more realistic fire scenarios given the characteristics of the structure under study, such as localised fires. The new generation of Eurocode 1 Part 1–2 introduces various localised fire models for structural components, considering their positions relative to flame exposure. This study employs localised fire models to assess the thermal-structural performance of the portal frame structures. Results indicate that unprotected steel structures do not meet the required fire resistance classifications under the prescriptive design approaches stipulated by the Italian Fire Prevention Code. However, when using physically-based fires within performance-based design approach, the anticipated failure time of the unprotected structures is significantly extended, possibly beyond the requirements depending on the performance objectives. This paper suggests that the application of fire protection materials can be optimized leading to more efficient and cost-effective fire safety designs.

## 1. Introduction

Single-storey buildings, particularly those employing portal frame systems, are widely used for industrial halls or retail building thanks to their cost-effectiveness, rapid assembly, and large clear spans. The storage of extensive combustible materials within these large spaces increases their vulnerability to fire incidents. In contrast, the large open spaces in such buildings can prevent the occurrence of flashover, therefore performance-based design approaches may benefit from utilizing localised fire models to more accurately simulate fire behaviour. Several studies [1–5] have been conducted to understand the behaviour of single-storey steel structures in fire conditions. Moss et al. [2] investigated the collapse behaviour of steel portal frames under fire conditions using finite element model. The numerical results indicated that providing rotational restraint in base connections may prevent sideway collapse. Obiala et al. [3] emphasized the importance of designing steel industrial halls to collapse inward during fire events. The inward collapse mode prevents structural elements from falling outward that can endanger the safety of firefighters and occupants during evacuation. Li et al. [5] performed experimental and numerical studies to identify various collapse modes such as column lateral, column buckling, overall inward and overall outward collapses.

Fire performance of steel single-storey structures can be assessed both according to the prescriptive and the performance-based design (PBD) approach [6]. The prescriptive approach is the traditional method for fire design of steel structures [7]. It requires compliance with design criteria outlined in building codes and standards that specify fire resistance ratings based on nominal fire curves and fire protection measures for specific building types and occupancies. PBD approaches are increasingly becoming popular for the design of steel structures, particularly in fire conditions [8–12]. Gernay [13] provided an overview of the performance-based design approach to structures in fire. The

* Corresponding author.
*E-mail address:* batuhan.der@unitn.it (B. Der).

https://doi.org/10.1016/j.jcsr.2025.110076
Received 5 September 2025; Received in revised form 19 October 2025; Accepted 28 October 2025
Available online 8 November 2025

choice of fire design approach for steel structures depends on the type of building, regional codes, building complexity, and stakeholder requirements [13].

The prescriptive design approach uses nominal fire curves, that represent the fully-developed compartment fire, to perform thermal analysis of steel structures. However, the occurrence of a fully-developed fire in large spaces is less likely due to the proportion of the fire load distribution and the highly ventilated volumes. Localised fires typically occur in large spaces, such as large industrial halls or retail enclosures [14]. Localised fires (pre-flashover fires) can lead to non-uniform gas distribution which causes large temperature gradients in structural members [15]. The mechanical response of steel structures under localised fires has been studied for, including: columns [16–20], beams [21–24] and single-storey structures [25–28]. These studies provided valuable insights into the behaviour of steel components and structures under localised fire conditions, highlighting the importance of considering such scenarios in performance-based fire design. Localised fire exposure can significantly endanger the stability of structures [14].

The severity of fire effects on steel structures can be mitigated through the application of protection measures. Prescriptive fire design may apply fire protection materials to steel members to satisfy the required fire resistance class. Intumescent coatings are extensively applied in steel structures to combine fire safety requirements with aesthetic considerations. Spray fire-resistive materials (SRFM) are also commonly used protection measures in steel structures due to effective protection and ease of use. Since this passive fire protection is costly, there is interest in understanding more precisely how much of it is required to achieve the desired performance under the anticipated design fires, rather than applying prescriptive ratings that deliver unknown level of safety. Performance-based fire design (PBFD) can lead to significant reductions in construction costs by allowing more rational use of fire protection materials in structures.

The second generation of Eurocodes, which is being finalised, includes natural fire models that can be used within a PBD approach. In particular, the new Annex C of EN 1991–1-2:2021 [29] introduces three primary localised fire models: Heskestad, Hasemi, and LOCAFI [30,31]. The Heskestad method can be employed to estimate the flame height and associated thermal conditions along the fire axis when the flame is not reaching the ceiling. If the flame impacts the ceiling, the Hasemi model is used to calculate the resulting heat flux to structural elements at the ceiling level. For localised fire scenarios where vertical structural members are not engulfed by flames, the LOCAFI model [30,31] is employed to assess the radiative heat flux from the fire to these members. According to EN 1991–1-2:2021 [29], localised fire models are applicable under specific conditions where diameter of the fire $\leq$10 m and rate of heat release of the fire ($Q$) $\leq$ 50 MW.

Therefore, this study provides a fire design methodology employing two main design approaches for portal frame structures. Unlike previous studies that rely primarily on standard fire curves, this work compares the thermal and structural performance under both prescriptive and performance-based fire design methodologies through detailed numerical simulations using different fire scenarios. The novel contribution of this paper lies in the application of the newly introduced localised fire models from the upcoming Eurocode 1 Part 1–2 to the fire design of single-storey steel structures with different occupancy types. The main purpose of this research is to determine whether a PBD approach, in the context of the 2nd generation of EN 1991–1-2, can mitigate the need for passive fire protection materials considering more realistic fire scenarios compared to standard fire curves.

## 2. Fire design methodology

According to Italian Fire Prevention Code (FPC) [32], the designer must first determine the required fire performance level for the structure based on its intended occupancy, then select the fire design approach, either the prescriptive approach or the performance-based design (PBD) approach [13]. In this study, the industrial hall corresponds to Performance Level II, while the retail building corresponds to Performance Level III, under both design approaches. Fig. 1 presents the flowchart for fire design of structures.

In prescriptive design approach, a standard temperature-time curve is selected to represent the fire exposure. The required fire resistance classification ($R_{time}$) is first determined based on occupancy and fire performance level, with national annexes (e.g., FPC [32]). The next step involves conducting thermal analysis using the selected curve to determine the temperature evolution in the structural elements. This is followed by a mechanical analysis to evaluate the structural response under elevated temperatures and to determine the failure time (FT). The FT is defined as the moment when the structural system either undergoes global instability, resulting in a collapse, or when the deformation of individual components exceeds the prescribed deflection limits, indicating a loss of load-bearing capacity. If the calculated failure time does not satisfy the required fire rating, fire protection materials may be applied to the structural components to enhance their load-bearing capacity under fire conditions. Subsequently, the thermal and mechanical analyses should be repeated to verify compliance with the fire resistance requirements.

The Italian FPC [32] permits the adoption of PBD for the fire design of steel structures. For single-storey industrial and retail structures, common objectives are safety of the building occupants (who can be evacuated relatively rapidly given the building layout) and avoiding an outward failure that would spread the fire and/or damage to adjacent structures. Application of a PBD begins with the determination of the fire performance level. Next, worst-case design fire scenarios are developed, considering fire location, fire load, and heat release rate (HRR). The design fire should be located beneath or adjacent to critical structural members to ensure safety under the most severe conditions [33]. Design fire loads and the rate of heat release can be estimated in accordance with relevant standards. Subsequently, the required fire performance (RFP) is evaluated based on the fire performance level and fire load. The PBD approach employs localised fire models for thermal analysis to determine the non-uniform temperature distribution on the structural components. Thermal analysis is then carried out under these scenarios, followed by the mechanical analysis to compute the structural failure time. If the calculated structural FT does not exceed the RFP, additional active fire protection measures may be implemented to change RSET (for performance level II) and the fire load (for performance level III) or enhance the structural load-bearing capacity.

## 3. Building prototype for the portal frame

A 25 × 49 m single-storey steel structure, with an enclosed indoor area of 1225 square meters, is selected as the case study. The portal frame comprises columns with an eaves height of 3.5 m, while the inclined rafters provide an overall frame height of 3.875 m at the roof apex. The structure is assumed to be situated in Italy and is analysed under two different occupancy types: an industrial hall and a retail building. The steel structure comprises composed portal frames interconnected by cold-formed purlins. The span of the portal frame is 25 m, and the spacing of columns is 7 m. The portal frame is hinged at the base in both principal directions, and the rafter-to-column joints are considered as fixed. Fig. 2 illustrates the three-dimensional structural model of the single-storey steel structure, featuring different structural elements composing internal and end frames. The end frames are composed of rafters made of IPE330A and columns HE300A; whilst the internal frames are made of IPE550 rafters and HE360A columns. The steel grade is S460. Roof and side purlins are modelled using Sigma 300 × 4 and Sigma 300 × 2.5 profiles, whose steel grade is S550GD + Z/ZM. To ensure lateral stability in the longitudinal direction, horizontal and vertical diagonal bracing members composed of 30 mm diameter round bars made of S235 grade structural steel are inserted into the building. In the analysed structure, haunches and stiffeners are incorporated at the

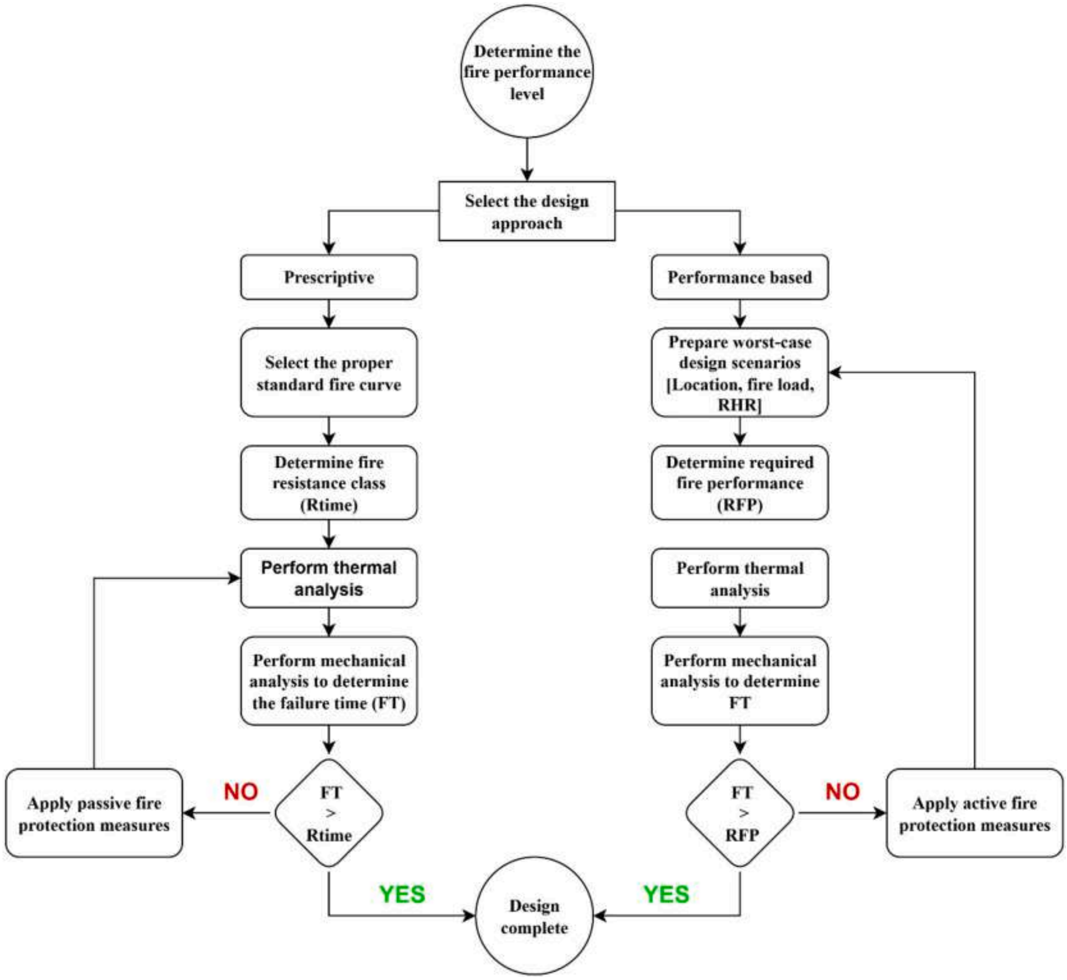


**Fig. 1.** Flowchart for the fire design of the structures.

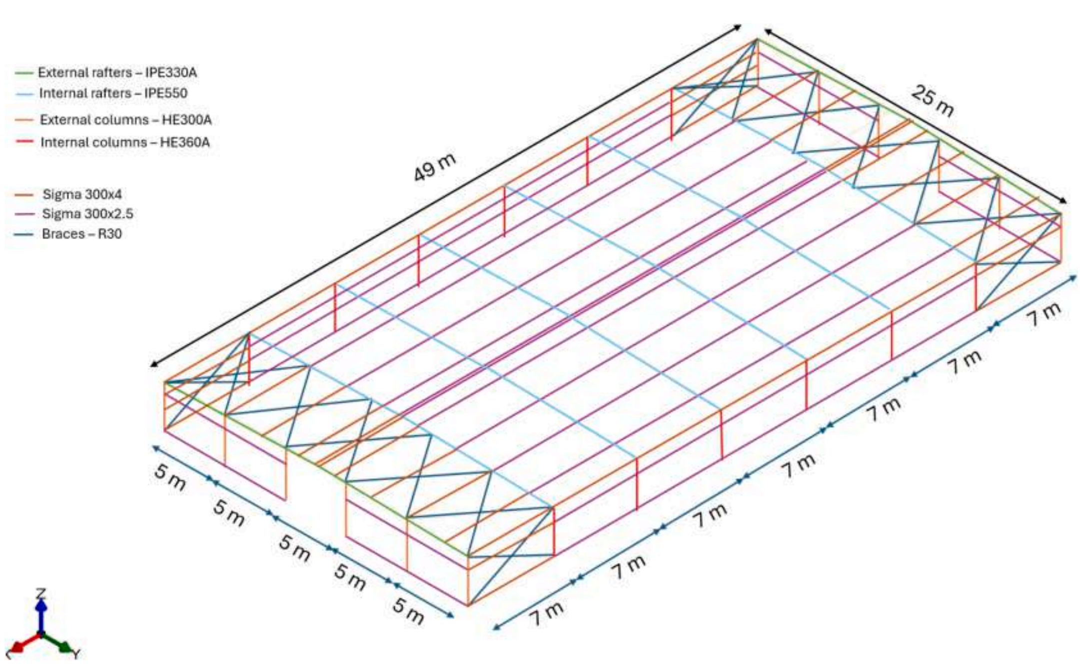


**Fig. 2.** Layout of the steel single-storey steel structure in SAFIR.

rafter-to-rafter and rafter-to-column joints to enhance moment resistance and stiffness.

Table 1 outlines the structural components of the analysed building, specifying the cross-sectional profiles and corresponding steel grades utilized for each member. In the numerical model, the roof and facade elements were not explicitly modelled; instead, their self-weight was considered and applied to the structure as permanent loads. The used profile for the steel roof design is the continuous deck type Hacierco 74S, with a gauge thickness of 0.63 mm. The sandwich panel Promisol S900 with a thickness of 120 mm was selected for the façade system.

## 4. Design fires

### 4.1. Fire design scenarios

The goal of this study is to compare the structural behaviour of single-storey buildings exposed to various fire scenarios. Both nominal and localised fire scenarios are used to assess the fire performance of steel structures. Localised fire scenarios are denoted using the format OT–FS#-MT, where *OT* represents the occupancy type (IH for industrial hall and RB for retail building), *FS#* refers to the scenario number as described in Fig. 3 and *MT* indicates the model type (WS is the whole-structure and PF is the portal frame).

#### 4.1.1. Nominal fire curve

EN 1991–1-2:2021 [29] allows designers to use nominal temperature-time curves to characterize the fire in the prescriptive design approach. The ISO 834 fire curve was chosen in this study because it specifies cellulosic fire load, which suits compartment fires. The temperature development of the ISO 834 fire curve is described as follows:

$$\theta_g = 20 + 345\log_{10}(8t+1) \tag{1}$$

where $t$ is the time in minutes. All structural components are assumed to be exposed to the standard temperature-time curve, as defined by the ISO 834 fire curve.

#### 4.1.2. Localised fire models

The effect of the fire location within the building was investigated using four localised fire scenarios, as shown in Fig. 3. Different fire scenarios were considered varying the position and intensity of the localised fires for different occupancy types. Localised fire scenarios were defined based on the presence of 10 tons of cellulosic material stored over an area of 50 $m^2$ within the industrial hall [30]. This storage corresponds to a circular fire with an equivalent diameter of approximately 8 m. The density of typical cellulosic materials ranges from 100 to 800 $kg/m^3$. Low-density cellulosic material ($\sim$100 $kg/m^3$) would be stacked about 2 m high in a 50 $m^2$ area, whereas high-density material ($\sim$800 $kg/m^3$) would form a much smaller stack, approximately 0.25 m (25 cm) high. Industrial halls typically have a wider distribution of combustible materials in large quantities compared to retail buildings. As a result, an 8-m fire diameter was adopted for fire scenarios within industrial hall, as shown in Fig. 3. In contrast, a 5-m fire diameter was assumed for fire scenarios used in the retail building. A fire load density of 1022 $MJ/m^2$, calculated in this study for the retail building at Performance Level III, over a 50 $m^2$ storage area is equivalent to roughly 3 tons of cellulosic material. This assumption accounts for lower fire load amount and the more limited spatial distribution of combustible materials generally stored in retail buildings compared to industrial halls. For the fire design scenario of the retail building, the stack height of cellulosic material over a 20 $m^2$ area ranges from approximately 0.075 m for high-density material to 0.6 m for low-density material.

**Table 1**
Components of the analysed steel framed structures.

| Component | Cross section [mm] | Grade |
|---|---|---|
| Internal columns | HEA 360 | S460 |
| External columns | HEA 300 | S460 |
| Internal rafters | IPE 550 | S460 |
| External rafters | IPE 330 A | S460 |
| Bracing Members | Circular Bars (∅30 mm) | S235 |
| Purlins & Side Rails | Sigma 300 × 2.5 & 300 × 4 | S550GD + Z/ZM |

Fig. 3 shows the locations of the fire ignition points for all fire scenarios considered in the WS model. Scenario 1 is positioned at the mid-span of the portal frame beneath the bracing system. This scenario examines the fire effect on bracing elements and adjacent columns. Scenario 2 is located adjacent to a column of the end frame and under the bracing. This scenario investigates structural fire performance, particularly in terms of asymmetric deformation. Scenario 3 is situated under internal rafters at the centre of the portal frame. Scenario 4 is positioned near an internal column at the centre of the portal frame. Scenarios 3 and 4 both study the thermal and mechanical behaviour of rafters, purlins and internal columns in areas with limited lateral restraint. In all four scenarios, the flame reaches the ceiling level, therefore detailed evaluation of structural elements located near the ceiling is required in thermal analysis. For the PF models, two different scenarios are used. IH-FS1-PF involves a fire located at mid-span, while IH-FS2-PF considers a fire located 4 m away from the column in the y-direction.

Fig. 4 illustrates the zones of application for localised fire models within performance-based fire design approach using SAFIR [34] software. The descriptions of the numbers in parentheses in Fig. 4 correspond to the structural components listed in Table 2. In this study, the flame reaches the ceiling in all fire scenarios. This study uses LOCAFI fire model with only a conical flame representation, as no vertical structural component is engulfed by the flame in any of the fire scenarios. The smoke layer accumulated beneath the ceiling is a significant factor in determining the appropriate fire model in Eurocode approach and analysis method. EN 1991–1-2:2021 [29] proposes a Hasemi fire model for structural components, affected by flame impingement, above a threshold height of *H/10* (where *H* denotes the distance the fire source and the ceiling) from the ceiling. However, EN 1991–1-2:2021 recommends a more refined approach, suggesting the combination of a two-zone model and a localised fire model for a more accurate estimation of temperature distribution in structural members, by considering the maximum effect at each location given by the two fire models. Therefore, in this study, the smoke layer height ($z_{smoke}$) was calculated using Ozone [35]. In the analysis method, $H^*$ represents the limit height for applying the Hasemi fire model in SAFIR [34] and is defined as the greater of the calculated smoke layer height or *H/10*, as specified in the Eurocode approach. Table 2 presents the main parameters and modelling methodology used for localised fire scenarios in, both the industrial hall and the retail building.

### 4.2. Quantification of design fires

#### 4.2.1. Fire loads

The design fire loads for an industrial hall are calculated based on the design example in Appendix D of the LOCAFI+ guide [30] using the following expressions:

$$q_f = H_i.M \tag{2}$$

where $H_i$ equals to 17.5 MJ/kg (the lower calorific value of the cellulosic material) and $M$ equals 10,000 kg (the mass of cellulosic material). These cellulosic materials are considered isolated from other combustible materials. EN 1993-1-2:2021 [29] does not provide values for fire load density for industrial halls. In this study, a fire load density of 3500 $MJ/m^2$ is assumed, which is consistent with the range of 80–4923 $MJ/m^2$ observed for production rooms in industrial halls, as presented in the handbook [36].

Annex E of EN 1991–1-2:2021 [29] provides methodology to

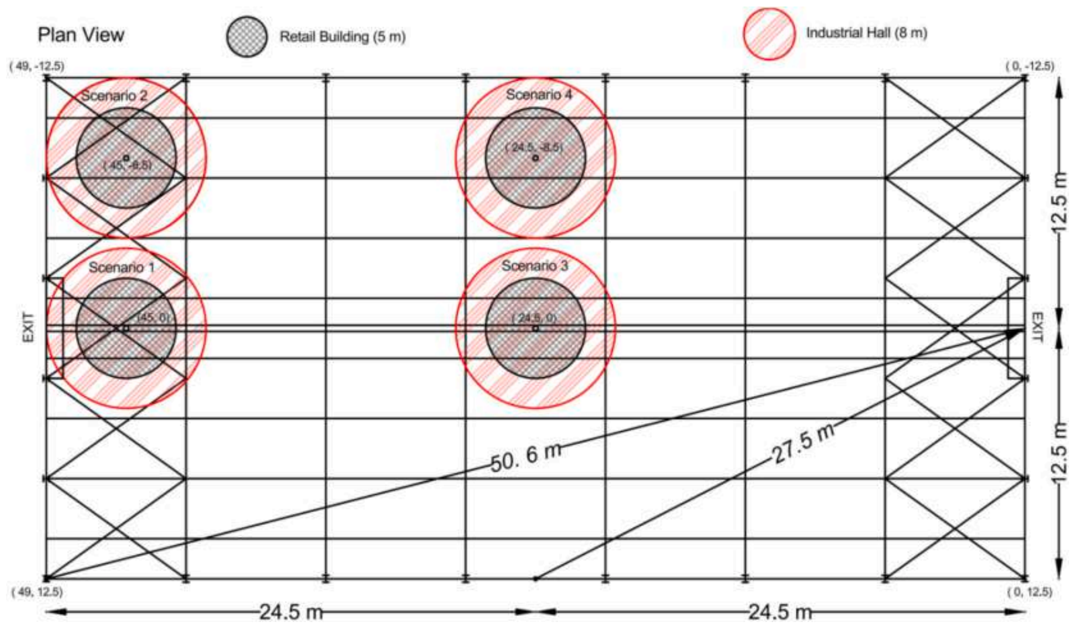


**Fig. 3.** Locations of the studied localised fire scenarios and evacuation distances in the entire structure.

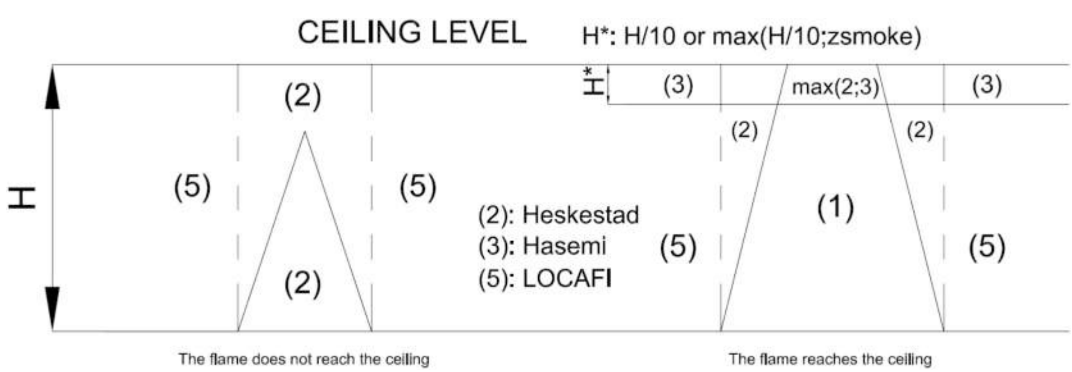


**Fig. 4.** Application domains of localised fire models based on EN 1991–1-2.

determine the design fire load for various building types. The value of the specific design fire load $q_{f,d}$ for retail building is evaluated using the following equation:

$$q_{f,d} = \delta_{q1}.\delta_{q2}.\delta_n.q_{f,k} \tag{3}$$

where $\delta_{q1}$ is a factor that takes into account the fire risk in relation to the size of the compartment, $\delta_{q2}$ is the factor that takes into account the fire risk in relation to the type of activity undertaken in the compartment, $\delta_n$ is the factor that takes into account the different fire prevention measures in the compartment and $q_{f,k}$ is the characteristic fire load. The gross floor area of the studied structure is 1225 $m^2$ (1000 $m^2 \leq A < 2500$ $m^2$), therefore $\delta_{q1}$ is taken as 1.4. Risk class II is accepted for retail building and $\delta_{q2}$ is 1.0. In accordance with the Italian FPC [32], the partial coefficients $\delta_n$ related to fire protection measures must be taken as unity when defining the natural fire curve. According to Appendix E of EN 1991–1-2 [29], the characteristic fire load $q_{f,k}$ for buildings used as commercial areas is 730 MJ/$m^2$. Based on this value, the design fire load for the retail building is calculated as 1022 MJ/$m^2$.

#### 4.2.2. Rate of heat release (RHR) curve

The RHR curve is defined in accordance with the Italian FPC [32] and EN 1991–1-2 [29] for both the industrial hall and retail building. A medium fire growth rate ($t_\alpha = 300$ s) is assumed for the industrial hall, with no active suppression systems. For the retail building, a rapid-fire growth rate ($t_\alpha = 150$ s) is adopted, and the fire is considered fuel-controlled due to sufficient ventilation. The maximum heat release rate $RHR_{max}$ is determined using the characteristic fire load ($q_f$), the fuel-covered area ($A_f$) and tabulated values of $RHR_f$ derived from Appendix E of EN 1991–1-2:2021 [29]. A design value of 1000 kW/$m^2$ for $RHR_f$ was adopted for industrial halls [30]. Although EN 1991–1-2 proposes an $RHR_f$ value of 250 kW/$m^2$ for retail buildings, a value of 500 kW/$m^2$ was adopted in this study to account for localised fire scenarios. The equivalent fire diameter ($D_f$) is calculated as a function of time using the following relation:

$$D_f(t) = \sqrt{\frac{4.RHR(t)}{\pi.RHR_f}} \tag{4}$$

where $RHR(t)$ is the total heat release rate of the fire at time $t$ (kW), which can be evaluated using the formula provided in EN 1991–1-2 [29]. Fig. 5 demonstrates the RHR over time for two different occupancy types: an industrial hall and a retail building. The RHR profile for the industrial hall exhibits a more severe fire scenario, with a rapid increase to a peak RHR of 50 MW at approximately 30 min, followed by a sustained plateau until 60 min, and then gradually decreasing until it ends at 100 min. In contrast, the retail building demonstrates a much less intense fire development, with the RHR peaking at only 10 MW around

**Table 2**
Description of the localised fire scenarios and the corresponding analysis methods.

| Occupancy | No | Physical Fire Scenario | | | | | Eurocode Approach (EN 1991–1-2) | Analysis Method |
|---|---|---|---|---|---|---|---|---|
| | | Fire[1] Position [m] | Positions of members | Flame Height | RHR[2] [MW] | Max D [m] | | |
| Industrial Hall | 1 | (45, 0) | No structural component inside the flame. There are vertical, horizontal and diagonal structural components near ceiling level ($z \geq H^*$) | Flame impacts the ceiling (Flame Height > Ceiling Level) | 50 | 8 | Annex C in EN 1993-1-2 proposes different heat fluxes for the following zones[3]: | Different localised fire models are applied in SAFIR.[4] |
| | 2 | (45, −8.5) | | | | | **(2)** For components engulfed by the flame or within a conical zone above the flame | No component engulfed by flame. |
| | 3 | (24.5, 0) | | | | | | |
| | 4 | (24.5, −8.5) | | | | | **(3)** For components at the ceiling level ($z \geq 0{,}9H$) if the flame reaches the ceiling | **HASEMI** for components near the ceiling level ($z \geq H^*$) |
| Retail Building | 1 | (45, 0) | | | 10 | 5 | | |
| | 2 | (45, −8.5) | | | | | **(5)** For components not directly exposed to flame or at the ceiling level | **LOCAFI** for column and braces on facade ($z < H^*$) where are not engulfed by flame or not near ceiling level |
| | 3 | (24.5, 0) | | | | | | |
| | 4 | (24.5, −8.5) | | | | | Clause 5.3.2 (4) recommends the combination of a 2-zone model and localised fire model | OZone evaluates the smoke layer elevation[5]. $H^* = \max(H/10; \underline{z_{smoke}})$ |

[1] Fig. 3 indicates the position of each fire scenario.
[2] Fig. 5 shows the RHR curve of fire scenarios for industrial hall and retail building.
[3] Fig. 4 exhibits the described zones.
[4] Fig. 4 depicts the application of fire models in SAFIR.
[5] Fig. 7 shows the smoke layer elevation

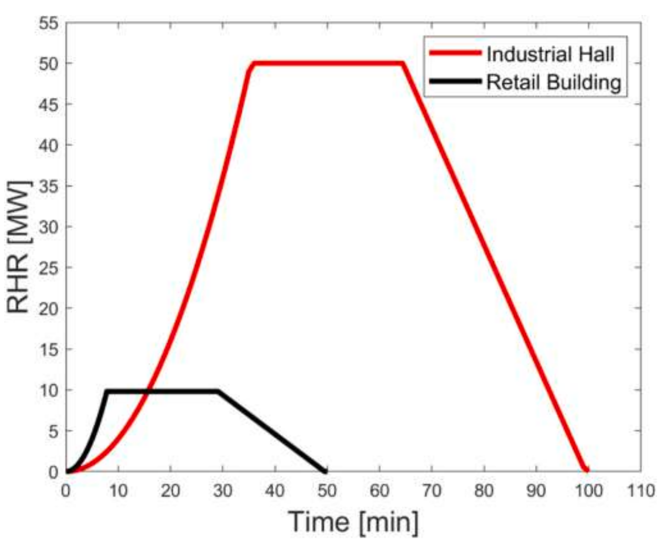


**Fig. 5.** RHR curve for industrial hall and retail building.

10 min, followed by a steady-state phase and a rapid decay completing within 50 min.

## 5. Fire design requirements

The required fire resistance duration for a structure is determined based on its occupancy type, the fire performance level, and the adopted design approach.

### 5.1. Determination of fire resistance class

The prescriptive design approach examines the fire performance of single-storey steel structure exposed to ISO 834 nominal fire curve. According to Italian FPC [32], the required fire resistance ratings for buildings may be established based on their occupancy type, and the corresponding performance level, the fire load density. For the industrial hall under study, a fire resistance rating of R30 is required to satisfy the criteria for Performance Level II. In the prescriptive approach, the Italian FPC requires that for Performance Level II the minimum fire resistance class must be at least 30 min or less depending on fuel load density. Given the fire fuel density of the analysed industrial hall, i.e. 3500 MJ/m$^2$, a minimum R30 requirement must be met. Conversely, retail buildings must achieve Performance Level III, corresponding to a fire resistance rating of R90 because the fire load density (1022 MJ/m$^2$) is less than 1200 MJ/m$^2$ in this study.

### 5.2. Determination of RFP

In Performance Level II for the industrial hall, the RFP is directly related to the Required Safe Egress Time (RSET), ensuring that the structure remains stable for the entire evacuation period. The load-bearing capacity must be guaranteed for a safety margin in terms of time, which is the maximum between twice the RSET and a minimum duration of 15 min, to satisfy the fire resistance requirements for Performance Level II. Italian FPC [32] presents a calculation method for RSET with reference to ISO/TR 16738:2009 [37] as follows:

$$t_{RSET} = t_{det} + t_a + \left(t_{pre} + t_{tra}\right) \tag{5}$$

where $t_{det}$ is the time from ignition to detection by an automatic system or first occupant to detect fire cues, $t_a$ is the time from detection to awareness/alarm, $t_{pre}$ represents the pre-movement time (from alarm to the beginning of evacuation movement), and $t_{tra}$ is the evacuation time. The detection time equals 300 s when the design fire reaches 1 MW and produces smoke and flames in sufficient quantity to be perceived by the occupants. This study assumes that the detection directly activates the general alarm of the building. Therefore, the time from detection to awareness/alarm is taken as 0 s.

PD7974–6:2019 [38] provides recommended values of time from alarm to movement based on the classification of building complexity and fire safety management systems. The maximum evacuation distance for each scenario is calculated as illustrated in Fig. 3. For Scenarios 1 and 2, the calculated evacuation distance is 50.6 m, while for Scenarios 3 and 4, it is 27.5 m. Annex D of PD 7974–6:2019 [38], the normal occupant walking speed is assumed to be 1.2 m/s. Consequently, the evacuation time is evaluated by dividing the maximum travel distance by the normal occupant speed. According to the Italian FPC [32], the available safe egress time (ASET) must be at least twice the RSET for Performance Level II. However, the required time cannot be less than 15 min in any case. In this study, the RSET for the industrial hall under four localised fire scenarios was calculated to be 7 min. Therefore, the industrial hall must remain structurally stable for at least 15 min in order to meet the fire performance requirements of Level II.

At fire performance level III, the RFP must be equal to the entire duration of the design fire. For retail buildings, the Required Safe Egress Time (RSET) does not need to be calculated, as the structure must meet Performance Level III fire resistance requirements. The fire resistance performance of the constructions must be verified on the basis of the design fire scenarios and the related design fires. Therefore, in order to demonstrate compliance with Performance Level III of fire resistance, it is necessary to ensure that the structure withstands the entire duration of the fire for all the design fire scenarios.

## 6. Numerical modelling

The nonlinear finite element software SAFIR [34] is used to investigate the thermal-structural response of steel structure under fire conditions. SAFIR [34] has been extensively validated through several studies, demonstrating its reliability in simulating the behaviour of steel structures exposed to elevated temperatures [20,39–42].

### 6.1. Thermal analysis

#### 6.1.1. Description of the thermal model

Two-dimensional thermal analyses have been performed to calculate the temperature distribution across each cross-section, as shown in Fig. 6. The software computes the temperature distribution across the cross-section over time providing fibre temperatures. The main inputs for thermal analysis in SAFIR [34] are thermal characteristics of materials and frontiers (temperature-time curve for nominal fire or flux-time curve for localised fire). The material properties involved in thermal analyses are the density, emissivity, the thermal conductivity and the specific heat of steel and the convective heat transfer coefficient, that were specified as for EN 1993-1-2 [43]. In particular, the emissivity of steel surfaces is taken as 0.7 in both design approaches. This study did not consider the potentially beneficial influence of hot-dip galvanizing [44] in reducing emissivity and delaying heat transfer to the steel.

#### 6.1.2. Prescriptive thermal model

The temperature distribution of each component was identical for the industrial hall and the retail building, as the same nominal fire curve was applied for both occupancies. Prescriptive design approach employs the ISO 834 fire curve to each structural component on four sides of cross-sections. The convective heat transfer coefficient equals 25 W/($m^2$.K), as prescriptive design approach uses nominal fire curve.

#### 6.1.3. Performance-based thermal model

In the performance-based design approach, the cross-sections are exposed to localised fire models including HASEMI or LOCAFI. The selection of fire models depends on orientation of the component and distance to the centre of localised fire. To apply the Hasemi fire model to structural components near the ceiling, the smoke-layer elevation was calculated using Ozone [35] for both occupancies, as shown in Fig. 7. In both the industrial hall and the retail building, ceiling openings were not considered in the Ozone simulations. For both occupancies, the boundary conditions at ambient temperature included wall openings corresponding to about 5.5 % of the total surface area. The openings were assumed to vary linearly with temperature, with the effective opening area at 400 °C considered to be five times larger than at ambient

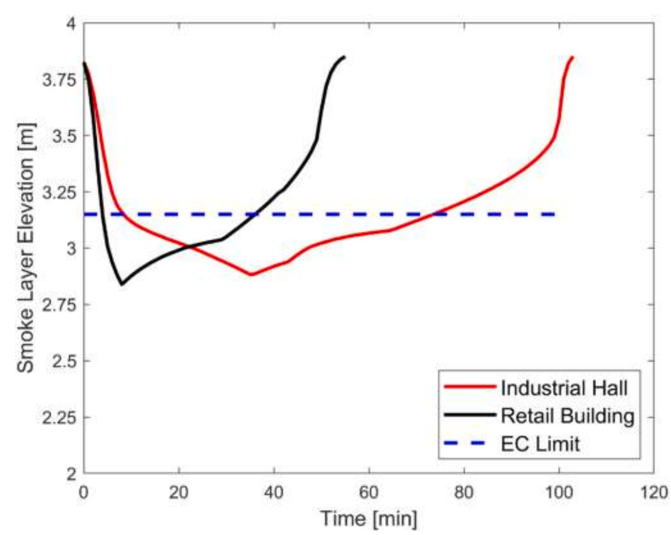


**Fig. 7.** Smoke layer elevation for industrial hall and retail building.

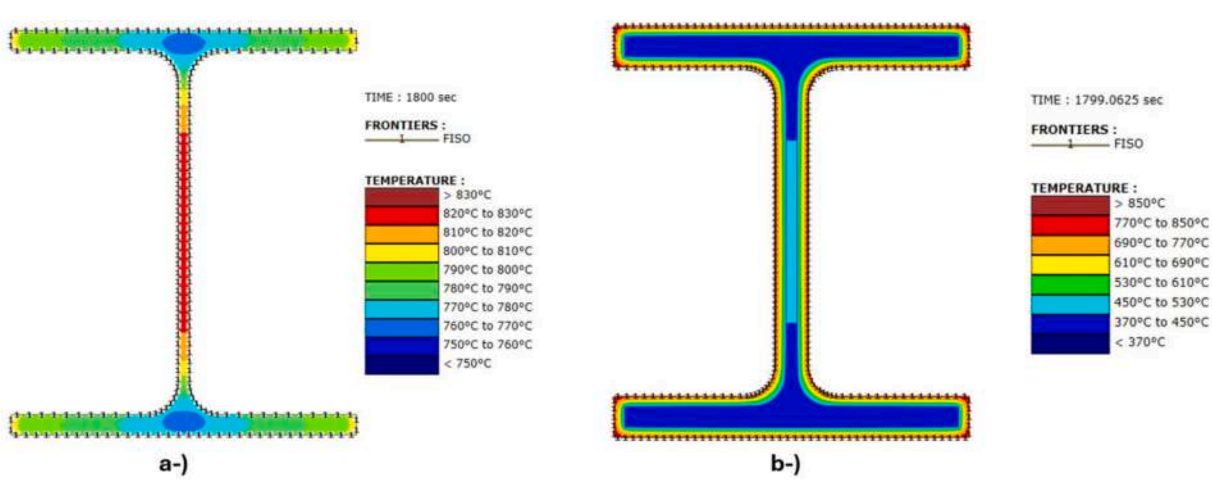


**Fig. 6.** Temperature trend for the HEA300 section exposed to ISO834 fire curve after 30 min: a) unprotected, b) protected.

temperature. However, at the early stages of the fire, the hot gas temperatures above the smoke layer are not significantly elevated. Therefore, the hot layer elevation was conservatively taken as 3 m in all numerical simulations. This value is lower than the recommended application limit of *H/10*.

Fig. 8 presents the temperature distribution in the HEA300 section exposed to localised fire models. The convective heat transfer coefficient is taken as 35 W/(m$^2$.K). Fig. 8a demonstrates that the cross-section exhibits higher temperatures on the face oriented toward the localised fire, as these surfaces receive the highest heat flux, whereas the opposite faces are subjected to lower thermal exposure. The cross-section in Fig. 8 is taken at a height of over 3 m along column (C6 illustrated in Fig. 10) under Scenario 1.

Four different fire scenarios (FS1 to FS4) applied to the whole-structure (WS) model are studied, as shown in Fig. 3. Recent studies have also emphasized that structures behave as thermal reservoirs during fire exposure, meaning that the overall thermal mass and energy balance play a critical role in structural resistance [45,46]. For IH-FS1-WS, a preliminary analysis was conducted to compare the full thermal model (all members) with the simplified model considering only the thermally critical members. Based on these results, in order to decrease the computation time, the members with temperatures below 100 °C are considered as cold members. Fig. 9 indicates hot and cold members for each fire scenario used in the PBD approach.

### 6.1.4. Results of thermal analysis

Fig. 10 illustrates the layout and numbering system of the columns (C1–C8) and rafters (R1–R5) used in the thermal and mechanical analysis of the single-storey steel structure. The results section adopts the same notation used for the fire scenarios, with the addition of the structural member code. Accordingly, results are expressed as OT–FS#-MT/M#, where the appended *M#* identifies the specific structural member (Column or Rafter) under consideration.

Fig. 11 presents the temperature evolution over time at various heights of a steel column subjected to standard ISO 834 fire curve and different fire scenarios. The curves labelled "Prescriptive" represent the temperatures predicted by the standard ISO 834 fire curve, corresponding to the prescriptive design approach. In contrast, the other curves (PBD H < 0.5 m, PBD 1.0 m < H < 1.5 m, etc.) correspond to performance-based simulations conducted at different vertical locations along the column. In each scenario, it is evident that the prescriptive approach predicts significantly higher temperatures (exceeding 900 °C) compared to the localised fire simulations, where temperatures vary based on height and proximity to the fire source. For instance, lower portions of the column (C1) experience minimal heating, especially in FS-IH-WS-3, where the curves remain below 200 °C throughout the 1 h duration. The upper portion of columns might have a much higher temperature than the lower portion because HASEMI fire model is applied for the part ($z > 3.0$ m) to consider hot smoke layer. These results illustrate that the prescriptive method may overestimate thermal demands on structural elements, whereas performance-based simulations capture the variability and localised nature of fire exposure, offering a more realistic estimation of temperature distribution along the column height.

Fig. 12 presents a comparative analysis of the thermal response of structural elements subjected to fire, derived from both the prescriptive (Pr) and PBD approaches across four different fire scenarios. The PBD models consider positional variation in fire exposure by assessing two horizontal positions (Y = 0 m and Y = -8.5 m) representing the location of nodes on the rafters. The results clearly show that the PBD approach predicts significantly lower temperatures for both rafter types in each scenario compared to the prescriptive approach.

Fig. 13 and Fig. 14 illustrate the temperature distribution over time (10, 20, and 30 min) on HEA300 and IPE550 profiles in the retail building under different fire exposure models. The comparison includes the prescriptive ISO 834 fire curve and localised fire models (LOCAFI and HASEMI) at various vertical positions from the flame centreline. In Fig. 13, the LOCAFI model is used at lower vertical positions than 3.0 m, while the HASEMI model is applied at a greater height. The temperature gradients are visualized through colour mapping on the cross-section of the steel profiles, showing increasing heat exposure with time and vertical proximity to the fire source. Fig. 14 presents a more detailed analysis for rafters using the HASEMI model under different fire scenarios (FS-RB-WS-3 and FS-RB-WS-4). It shows temperature distributions at multiple horizontal positions. The thermal response of the section is illustrated as a function of both time and different horizontal distance from the flame centreline.

## 6.2. Mechanical analysis

### 6.2.1. Description of models and assumptions

This study investigates the fire performance of single-storey steel structures under two different occupancy types. Following the thermal analysis, the mechanical study was conducted at two modelling levels: a whole-structure (WS) model and a portal-frame (PF) model in SAFIR [34]. The temperature distribution across each cross-section of the component is derived from the thermal analysis. The beam elements are used to model the structural members. To accurately simulate the structural collapse behaviour and address convergence challenges associated with static analysis, a dynamic analysis is employed. This

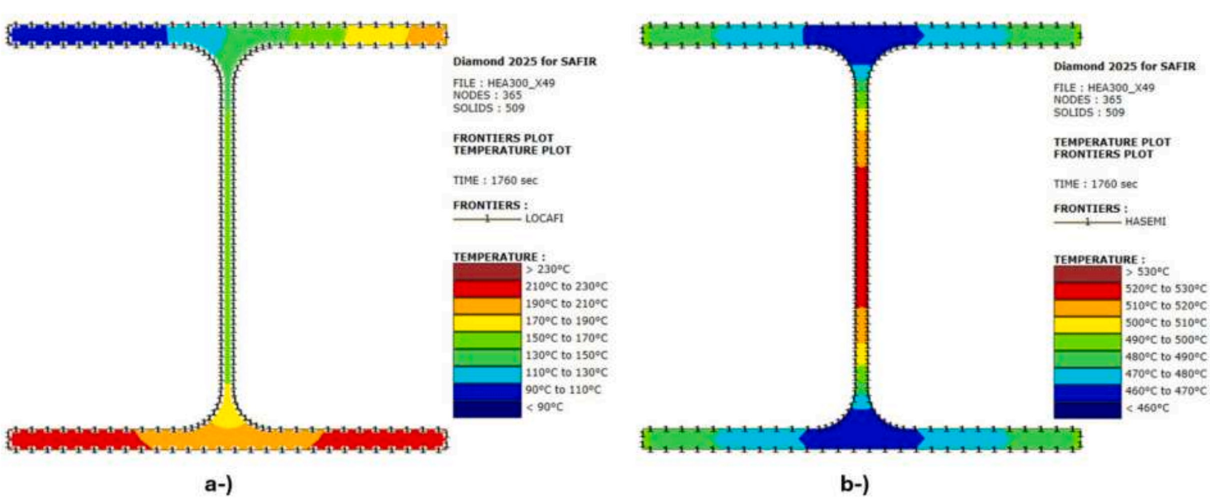


**Fig. 8.** Temperature trend for the HEA300 section after 30 min under Scenario 1: a) LOCAFI model, b) HASEMI model.

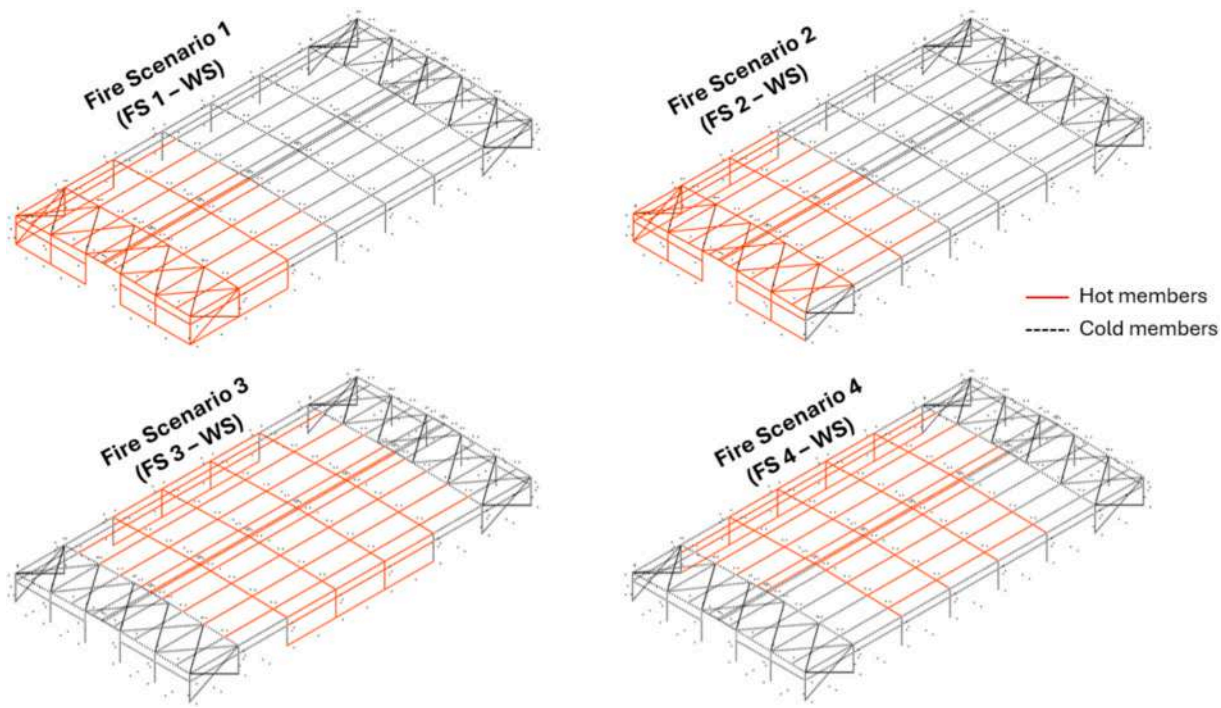


**Fig. 9.** Illustration of hot and cold structural members in industrial hall model.

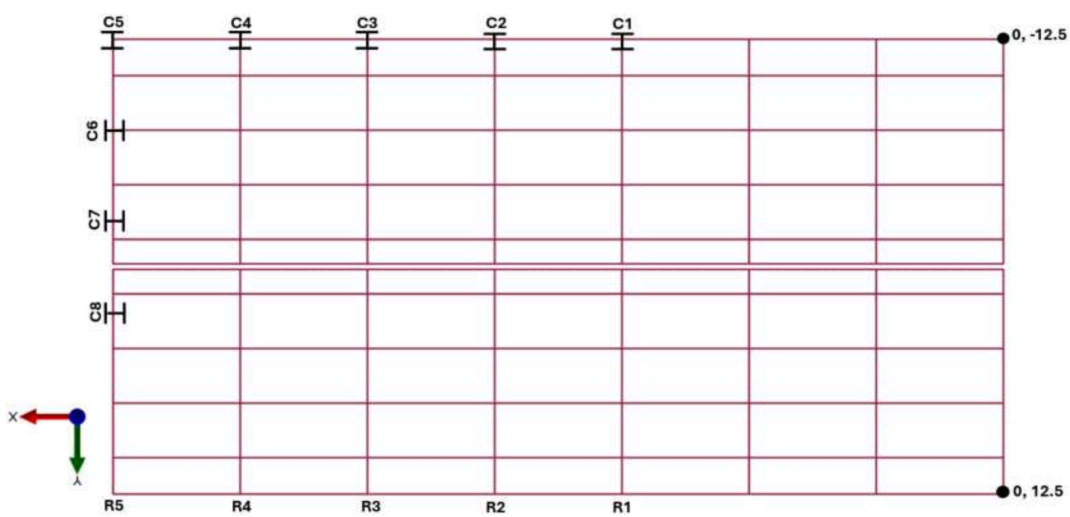


**Fig. 10.** Schematic diagram of the structure model.

approach is particularly effective in capturing the nonlinear response of structures under fire conditions. The roof was not included in the analysis, as it was assumed to provide no significant stabilizing effect on the purlins.

Figs. 15 and 16 illustrate the structural models developed for the mechanical analysis in this study. The whole-structure model comprises all primary and secondary structural components, including rafters, columns, braces, and purlins, whereas the portal frame (PF) model includes only the rafters and columns. The haunches were not explicitly modelled in the numerical analysis, as the frame was idealized using 3-D beam elements with rigid joints. This assumption therefore reproduces the increased rotational restraint and the associated moment amplification due to restrained thermal expansion during the early stages of fire exposure. A three-dimensional structural analysis was conducted for the portal frame to account for possible out-of-plane buckling phenomena.

Torsional and warping deformations are significant factors in determining the fire performance of steel structures composed of open sections, where torsional effects play an important role in the load-bearing capacity, particularly in cases of lateral-torsional buckling [47,48]. The degradation of the elastic shear modulus $G$ of the material due to high temperatures may result in a reduction in torsional stiffness $GJ$. Consequently, modelling the structure with beam elements while assuming a constant torsional stiffness could result in inaccurate predictions, particularly in scenarios involving failure due to lateral-torsional buckling. SAFIR [34] calculates elastic torsional stiffness as a temperature-independent parameter. In order to consider the effect of temperature on torsional stiffness, the user can manually reduce the torsional stiffness, for instance by a factor of 10. In the WS model, three different cases (listed in Table 3) were investigated to assess the effect of torsion and warping on the fire performance of single storey steel structures.

Table 4 lists four simulation cases for the PF model. These cases are

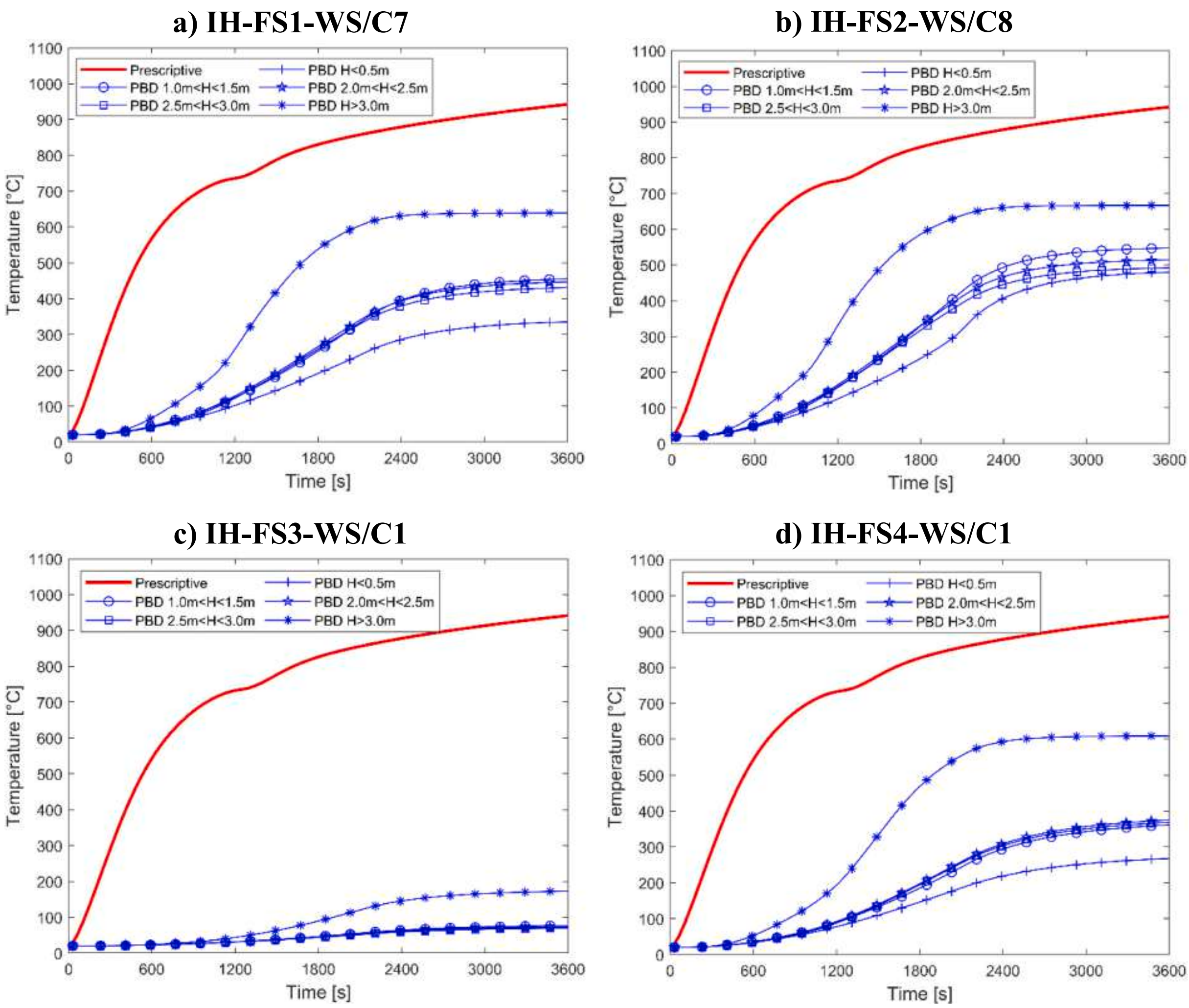


**Fig. 11.** Comparison of thermal responses of columns under fire exposure using prescriptive and performance-based design approaches for four localised fire scenarios.

used to perform comprehensive parametric study to assess the fire performance of a steel portal frame under varying fire scenarios, material properties, and boundary conditions. In PFd, the analysis considers a scenario where no equivalent imperfection loads are applied to the beam, meaning no out-of-plane loads are imposed on the portal frame. The PF model was developed specifically to evaluate the fire performance of structures intended for industrial hall occupancy.

### 6.2.2. Material models

The STEELEC3EN material model [43] in SAFIR is used to for the rafters, columns and braces and it follows the provisions of EN 1993-1-2 [43]. The purlins were modelled by STEELSL material [49], which is specifically designed for simulating slender steel sections, that may exhibit local instabilities, using beam finite elements. The reduction factors for mechanical properties of steel at elevated temperatures are adopted from EN 1993-1-2 [43]. It is generally accepted that the yield strength of steel fully recovers after being heated, as long as the maximum temperature of the material does not exceed a certain limit. In this work, the irreversibility of steel resistance is taken into account once the temperatures above 600 °C are reached, assuming a rate of decrease of the residual strength $\partial f_{y,r}/\partial T_{max} = 0.3\ MPa/K$. The section and material information of steel components are listed in Table 1.

### 6.2.3. Boundary and loading conditions

Boundary conditions are defined by restraining all translational degrees of freedom at the base of the columns, while rotational degrees of freedom are released to represent pinned connections for both models. Braces are modelled as pinned with released end rotations in the WS model. The portal frame is restrained in the out-plane direction to consider the effects of purlins, as shown in Fig. 15.

In structural models, the load combination selected to assess the fire performance of steel single storey structure was determined according to the Italian Technical Standards for Construction [50]:

$$E_d = G_1 + G_2 + P + A_d + \psi_{21} Q_{k1} + \psi_{22} Q_{k2} \quad (5)$$

where $G_1$ and $G_2$ are permanent actions including self-weight structural and non-structural components, $P$ is prestressing actions, $A_d$ is accidental actions, $Q_{k1}$ and $Q_{k2}$ are characteristics values of variable actions and $\psi_{21}$ and $\psi_{22}$ are quasi-permanent combination factors for variable actions. This study does not consider the wind and snow load acting on the structure during the fire, as EN 1990 [51] defines fire as an accidental design situation and the Italian National Annex specifies a combination factor of $\psi_2 = 0$ for wind load in the fire situation. Therefore, only self-weight of rafters, columns, braces, purlins, continuous roof steel deck (Hacierco 74S) and sandwich panel system (Promisol S900) are taken into consideration for mechanical response of the structure exposed to fire in the WS model. The PF model considers the self-weight of the modelled components. Additionally, vertical point loads representing the self-weight of the purlins were applied at their connection points to the portal frame.

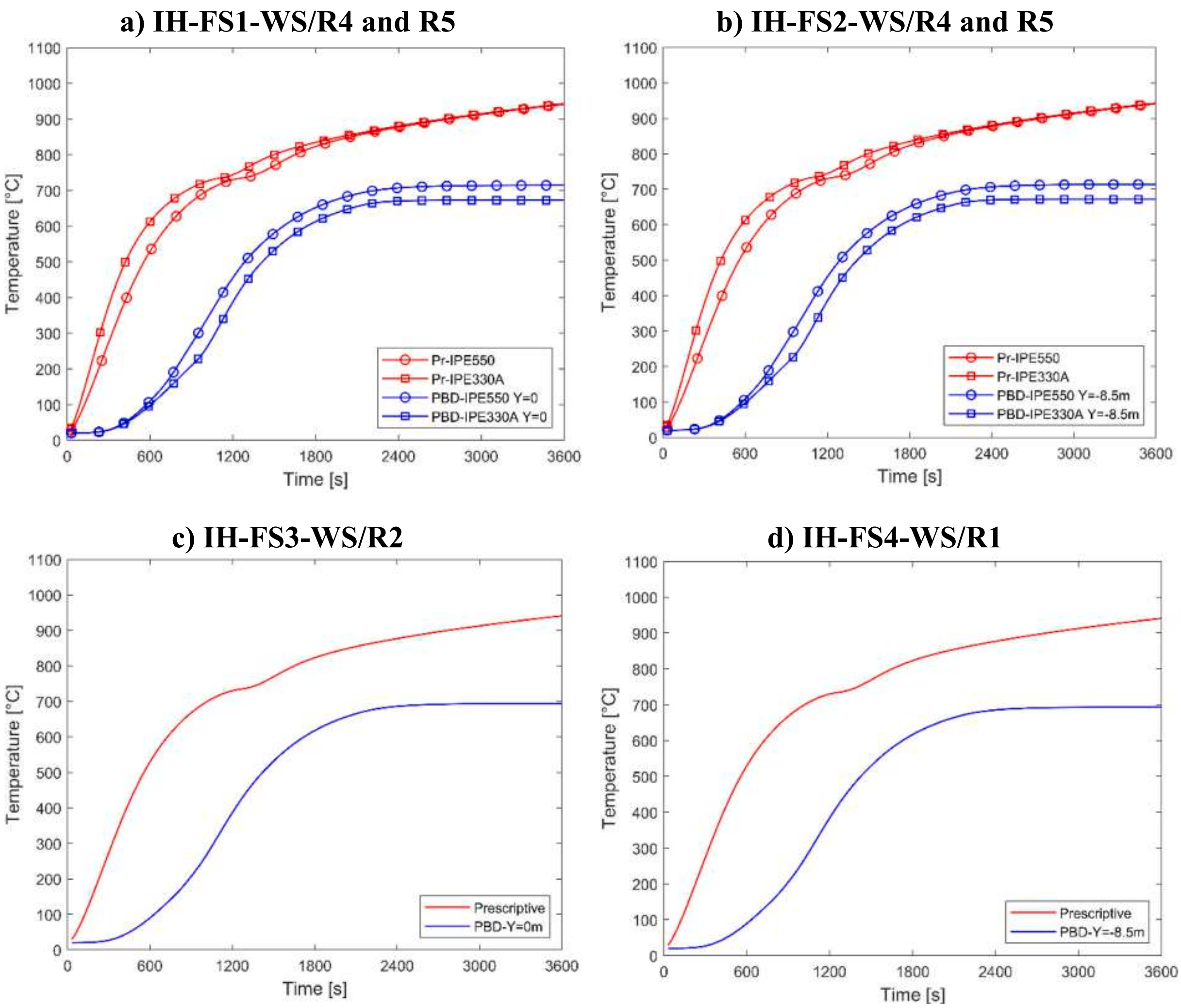


**Fig. 12.** Comparison of thermal responses of rafters under fire exposure using prescriptive and performance-based design approaches for four localised fire scenarios.

To account for global and member imperfections, equivalent horizontal forces are applied in accordance with EN 1993-1-1:2022 [52]. These forces reproduce the influences of global imperfections in the frames and bracing systems, and local imperfections in individual members such as rafters and braces. The applied equivalent forces and their corresponding affected members are presented in Table 4.

### 6.2.4. Analysis method

This section outlines the methodology for the mechanical analysis of single-storey steel structures. As discussed in Section 2, prescriptive design and PBD approaches are used to meet the fire design requirements. Two occupancy types are analysed (industrial hall and retail building) to investigate fire behaviour of the structures at two levels of analysis (WS and PF models). For the mechanical analysis, the nomenclature was adapted to the format OT–FS#–MTc, where *c* denotes the case identifiers described in Table 3.

In prescriptive design, both models (WS and PF) are exposed to the standard ISO 834 fire curve. The mechanical analysis is independent of the occupancy type, and the failure times obtained from the analyses are compared with the required fire resistance classifications.

The PBD approach, on the other hand, relies on fire scenarios that vary depending on the occupancy type and the level of structural modelling. Both WS and PF models are subjected to their corresponding fire scenarios, which are detailed in Section 4.1.2. For the industrial hall, the mechanical behaviour is analysed using both the WS and PF models. Parametric studies are conducted at both modelling levels to evaluate the influence of key parameters on the fire performance, as described in Section 6.2.1. The fire performance of the industrial hall is then compared between the WS and PF models. Finally, the retail building occupancy is investigated using the WS model to complete the mechanical analysis phase. Table 5 summarizes the structural models and corresponding fire scenarios considered for each occupancy type under both the prescriptive and PBD approaches.

### 6.2.5. Results and discussions

This section presents the fire behaviour of the single-storey steel structures using both the prescriptive and PBD approaches. First, the fire resistance of the structures is evaluated using the PFb and WSa models under the prescriptive approach, followed by a comparison of their responses. Subsequently, the PBD approach is applied to the industrial hall, where the effects of varying parameters are investigated using the PF model and compared with the WS model. The WS model for the industrial hall is further analysed to illustrate the failure time under three different cases. Finally, the PBD analysis of the retail building is presented based on the WS model results.

The portal frame, when exposed to the ISO 834 nominal fire curve, collapsed after 1009.7 s (approximately 16.8 min), ensuring a fire resistance of R15. Therefore, the minimum required resistance was not achieved for both occupancies. The whole structure under the ISO 834 standard fire curve collapsed after 1047s (approximately 17.5 min) with an inward collapse mechanism, ensuring a fire resistance of R15 and not satisfying the performance levels II and III. Fig. 17 indicates the global

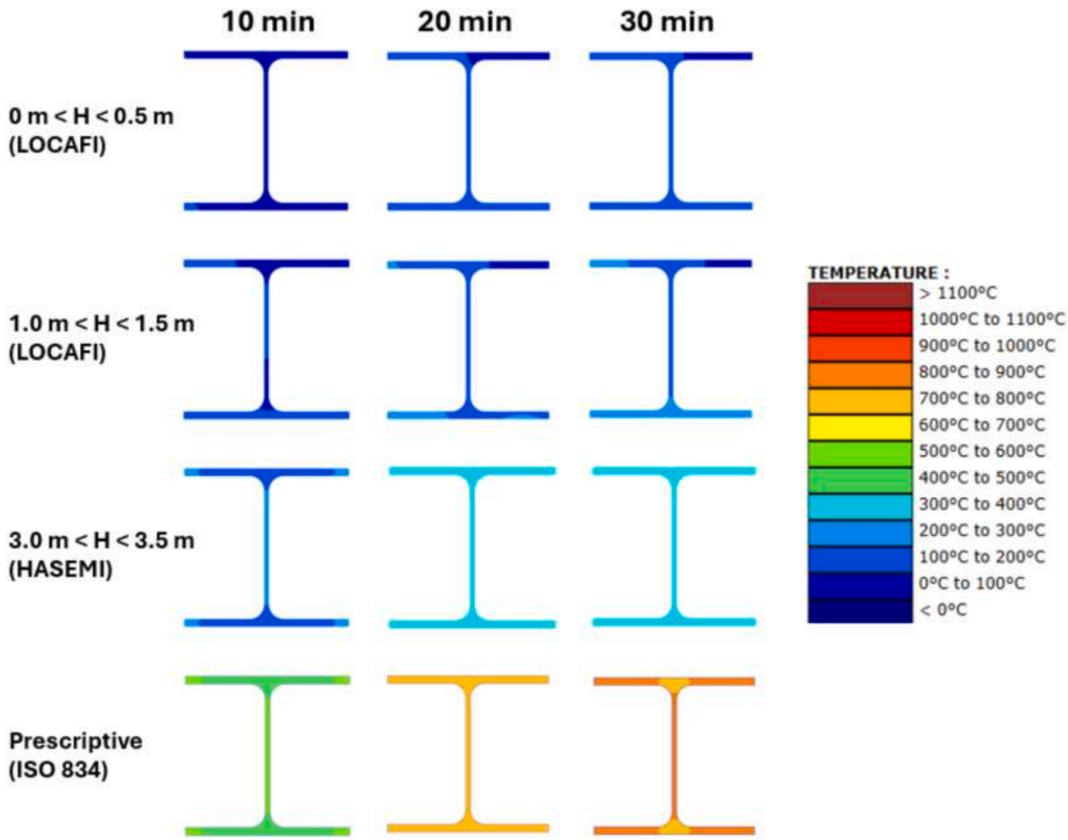


**Fig. 13.** Temperature distribution on HE300A (C5) steel section under RB-FS2-WS and nominal fire curves.

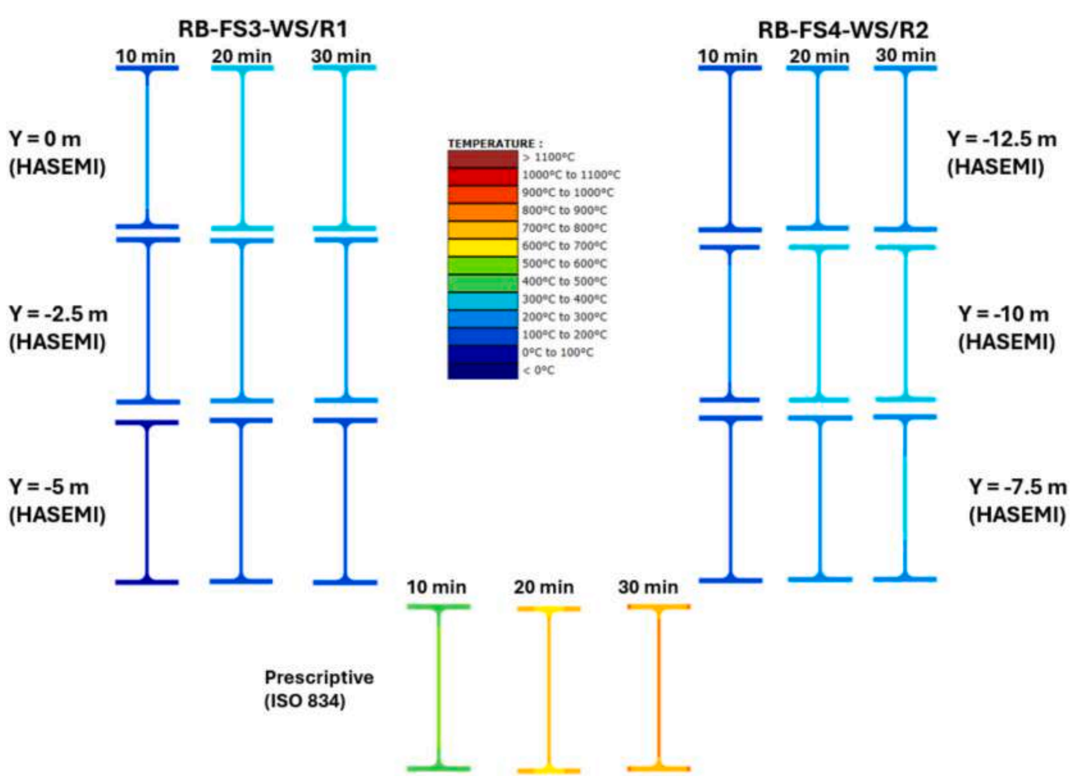


**Fig. 14.** Temperature distribution on IPE550 (R1 and R2) steel section under different fire scenarios.

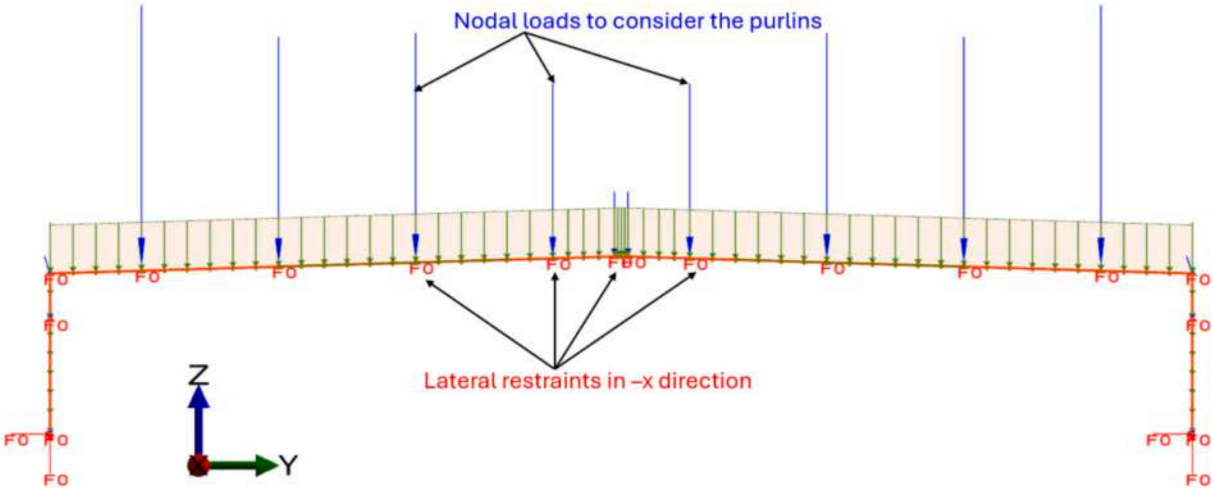


**Fig. 15.** Portal Frame Model.

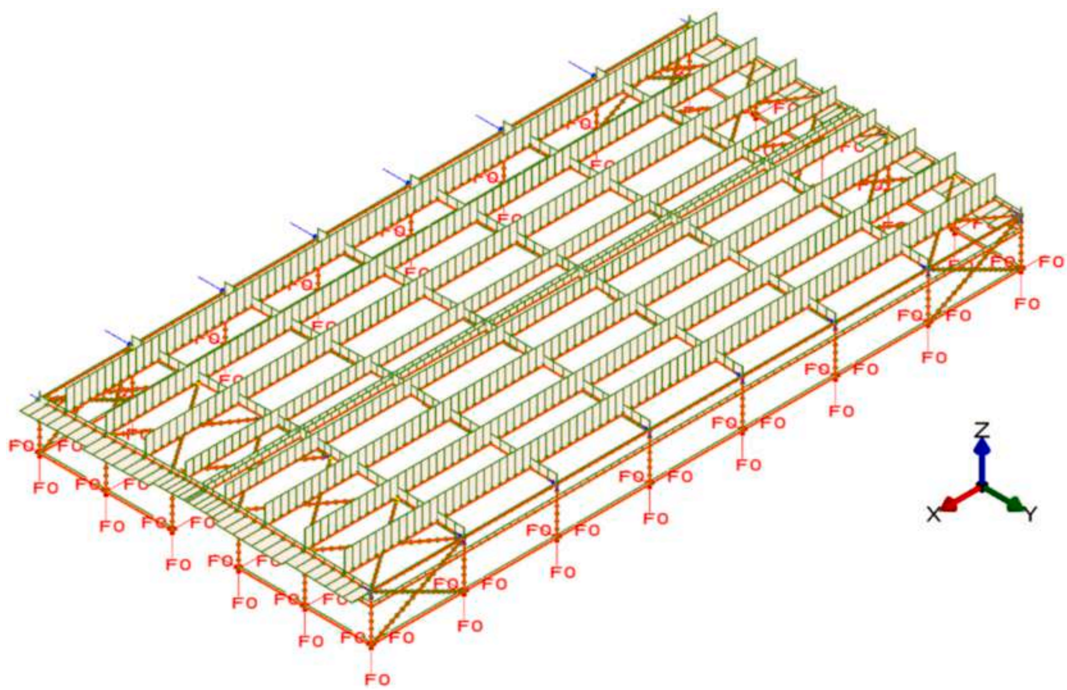


**Fig. 16.** The whole structure model.

**Table 3**
The description of cases for model types.

| Model Type | Cases | Torsional Stiffness | Warping | Steel Grades for Columns and afters | Reversibility of Steel Properties | Representation of Purlins |
|---|---|---|---|---|---|---|
| | a | GJ/10 | Restrained | | | |
| WS | b | GJ/10 | Free | S460 | Irreversible over 600 °C | Explicit |
| | c | GJ | Restrained | | | |
| | a | | | S460 | Fully reversible | Lateral restraints (Ux = 0) at purlins locations |
| PF | b | GJ/10 | Restrained | S460 | Irreversible over 600 °C | Lateral restraints (Ux = 0) at purlins locations |
| | c | | | S355 | Irreversible over 600 °C | Lateral restraints (Ux = 0) at purlins locations |
| | d | | | S460 | Irreversible over 600 °C | No lateral restraints at purlins locations |

**Table 4**
Summary of imperfection loads in the mechanical models.

| Imperfections for | Equivalent Forces [N] | Equivalent Forces [N/m] | Affected Member | Model Type |
|---|---|---|---|---|
| Global analysis of frames | 420 | – | Internal Columns | WS and PF |
| | 140 | – | External Columns | WS |
| Global analysis of bracing systems | – | 2661 | External Rafters | WS |
| Members | – | 230 | Braces | WS |
| | – | 238 | Internal Rafters | WS and PF |
| | – | 238 | External Rafters | WS |

**Table 5**
Overview of structural models.

| Occupancy | Prescriptive Approach | PBD Approach | |
|---|---|---|---|
| | Model Type | Model Type | Fire Scenarios |
| **Industrial Hall** | WSa | WS(a-c) | IH-FS(1–4)-WS |
| | PFb | PF(a-d) | IH-FS(1–2)-PF |
| **Retail Building** | WSa | WSa | RB-FS(1–4)-WS |
| | PFb | – | – |

failure mode of both models at the failure time.

Fig. 18a plots the vertical displacement at the centre of the rafter (R2), comparing the results obtained from the WSa model (node 113) and the PFb model (node 13). Both models exhibit a similar deformation trend. The displacement in the WSa model reaches a peak slightly after the PFb model due to the additional restraint and load distribution present in the WSa model. Fig. 18b presents the horizontal displacement at the top of the column (C2) for both the WSa (node 79) and the PFb model (node 3). The WS model shows a more restrained response, again highlighting the beneficial effect of global structural interaction and redundancy in resisting lateral deformations. The PFb model demonstrates good agreement with the WSa model in predicting both vertical and horizontal deformations under fire exposure. Therefore, while the PFb model provides a computationally efficient tool for preliminary assessment, the WSa model is recommended for detailed evaluation of structural performance in fire conditions.

Table 6 summarizes the structural performance of the PF models (only for industrial hall occupancy) subjected to localised fire exposure under two scenarios. Four cases (described in Table 3) were evaluated to assess the influence of varying fire characteristics, steel material properties, and boundary conditions on the structural response. In the early stage of a fire, thermal expansion causes the rafter to move upward, pushing the top of the columns outward. When sufficient lateral restraint is present and the material degradation in rafter increases further, the rafter experiences downward deflection which pulls the top of the columns inward due to the catenary action. This moment is called as start of downward deflection in Table 6. This mechanism ensures that the portal frame will collapse inward. In IH-FS1-PF, all cases exhibited the initiation of downward deflection between approximately 64.9 and 65.25 min, with no complete structural failure observed. Conversely, IH-FS2-PF demonstrated earlier onset of downward deflection collapse, ranging from 22.8 to 27.2 min, and subsequent failure times between 29.1 and 35.3 min. The material degradation, steel grades and the boundary conditions did not have a significant influence on the critical moments for portal frame models in IH-FS1-PF. However, in IH-FS2-PF the effect of steel grade and restraints becomes more visible. PFa and PFb display nearly identical behaviour, while PFc (S355 steel) shows earliest downward deflection, and PFd (no lateral restraints) experiences the earliest failure time.

Fig. 19 illustrates the displacement curves of the PF model for all cases under the two fire scenarios. In IH-FS1-PF, both the column top displacement in the y direction (a) and the rafter midspan displacement in the z direction (b) follow nearly identical trends across all cases. This confirms that variations in the assumed steel properties (reversible vs. irreversible after 600 °C), steel grade (S355 vs. S460), and boundary conditions have negligible influence when the fire is less severe. In contrast, under IH-FS2-PF, these parameters play a more significant role. While PFa and PFb exhibit almost identical responses despite different steel property assumptions, PFc (S355 steel) demonstrates earlier loss of stiffness and shorter failure time, and PFd (no lateral restraints at purlin locations) shows the most pronounced displacements and the earliest collapse. These results highlight that material degradation above 600 °C and the availability of lateral restraints are the governing factors for structural performance under severe localised fire exposure. These findings highlight the significance of incorporating realistic fire scenarios and structural conditions in performance-based fire design to accurately predict structural behaviour under fire exposure.

Fig. 20 illustrates the failure modes and corresponding collapse times of the industrial hall under localised fire exposure for four scenarios and three cases. In all cases of IH-FS1-WS, the industrial hall collapses due to the loss of strength and stiffness in the external portal frame comprising IPE300A rafter and HE300A columns. Notably, the roof bracings and purlins situated near the localised fire reach failure prior to the portal frame. Consequently, the portal frame undergoes collapse through an out-of-plane mechanism. In IH-FS2-WS, the structure is triggered by the failure of the HE300A lateral column adjacent to the localised fire, again

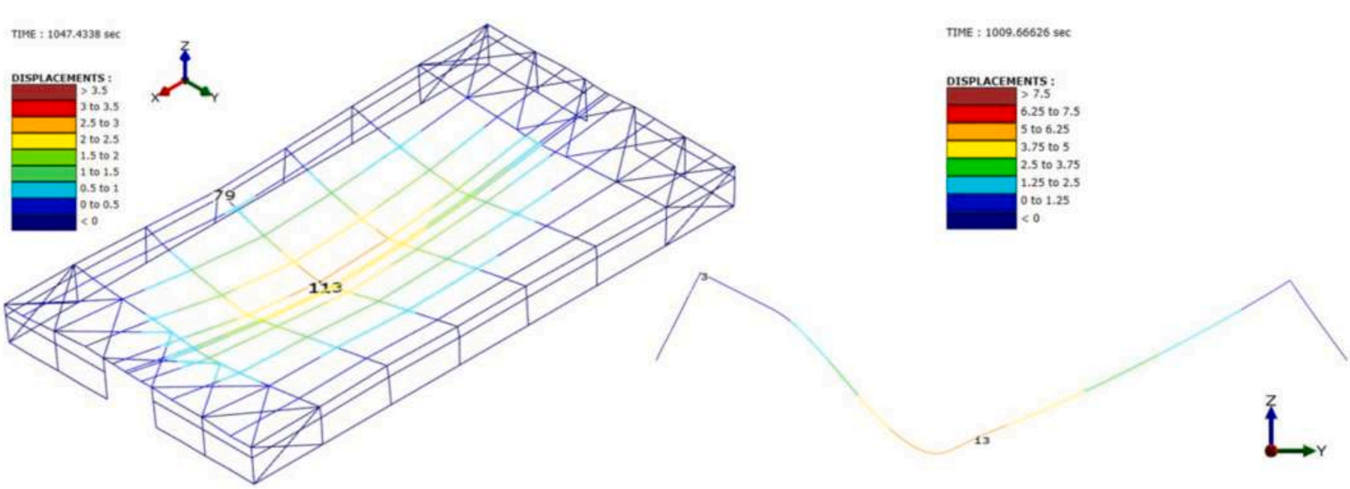


**Fig. 17.** Failure mode of the full structure and portal frame models in prescriptive design.

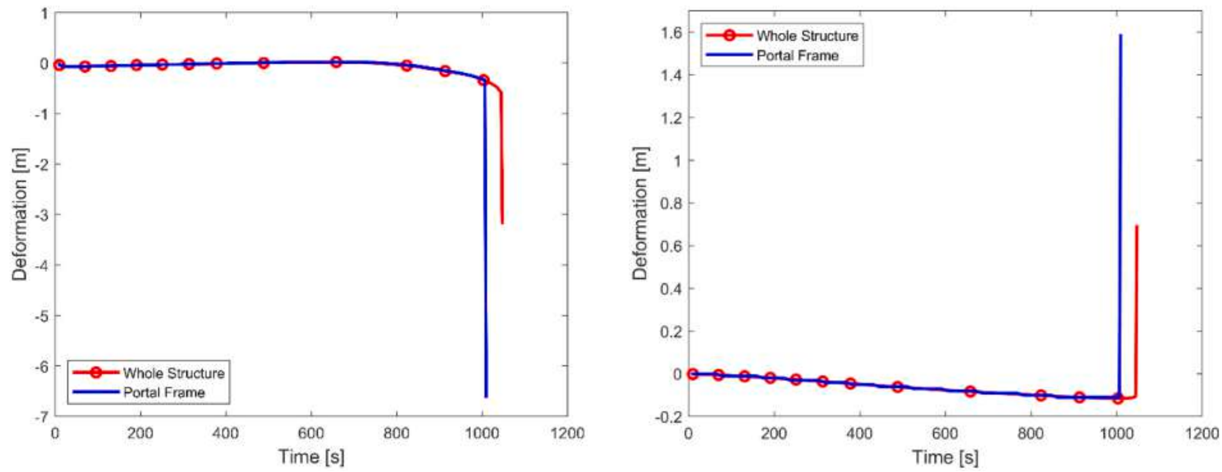


**a) Centre of the rafter (R2)** **b) Top of the column (C2)**

**Fig. 18.** Comparison of deformation between the WS and PF model for a) rafter and b) column.

**Table 6**
Performance-based fire design results for portal frames under two fire scenarios.

| Models | IH-FS1-PF | | IH-FS2-PF | |
|---|---|---|---|---|
| | Start of downward deflection [min] | Failure time [min] | Start of downward deflection [min] | Failure time [min] |
| PFa | 65.1 | No collapse | 24.8 | 33.5 |
| PFb | 64.9 | No collapse | 24.8 | 33.5 |
| PFc | 64.9 | No collapse | 22.8 | 30.9 |
| PFd | 65.25 | No collapse | 24.8 | 29.1 |

exhibiting an out-of-plane collapse mechanism. In IH-FS(3–4)-WS, the structure does not experience collapse because the fire is not directly influencing its critical load-bearing components. However, the purlins near localised fire exhibit significant deformations in both the lateral (y-direction) and vertical directions. The lack of effective lateral restraint leads to these large out-of-plane deflections, since the roof system was not explicitly modelled in the analysis. The failure criterion in the numerical model was defined as a deflection limit of *L/20*. As a result, the analysis is terminated upon reaching this deflection limit at the failure time for IH-FS(3–4)-WS as illustrated in Fig. 20. IH-FS4-WS shows slightly faster deflection (27.6–28.5 min) compared to IH-FS3-WS (31.9–33.6 min), possibly due to fire location or structural response. WSc provided the highest failure time for the structure in all scenarios. In Section 5.2, the RSET value is calculated as 15 min for Fire Performance Level II. As the industrial hall collapses later than 15 min under all scenarios and cases, it meets the criteria for Fire Performance Level II. These results indicate that torsional stiffness and warping at joints may have an effect on the structural response in fire. Thus, it is essential to adopt appropriate modelling assumptions. For instance, when lateral-torsional buckling governs the mechanical response, full torsional stiffness may be an unconservative assumption and reducing it can provide a more realistic representation a viable option. Moreover, depending on the joint features, e.g. for moment connections, warping may be restrained, whereas for pinned connections free warping represents a better assumption.

Fig. 21 presents a parametric investigation into the deformation behaviour of critical structural components under IH-FS(1–2)-WS. The deformation-time curves for the midspan of the rafter (R5) in the z-direction and the top ends of columns (C4, C6, and C7) in the y-direction are depicted, as these locations were selected based on their proximity to the fire-affected regions and their structural significance. The results demonstrated that the combination of reduced torsional rigidity and free warping results in larger deformations. It highlights the critical importance of connections on the fire performance of structures.

Fig. 22 provides a comparative study between the global structural response of the WS model (IH-FS(3–4)-WS) and the PF model (IH-FS (1–2)-PF), respectively. The deformation of the rafters is presented at the midspan in the z-direction, while the deformation at the tops of the columns is shown in the y-direction. In IH-FS1-PF, the portal frame model does not exhibit global collapse throughout the fire exposure duration. However, when analysing the WS model (under IH-FS3-WS), which includes secondary elements such as purlins, it is observed that the purlins located directly above the fire reach their deflection limits (*L/20*) significantly earlier (around 32 min) than the total fire duration of 100 min. In IH-FS2-PF, the portal frame model predicts structural failure approximately around 30 min into the fire event. In contrast, the WS model (under IH-FS4-WS) indicates that the purlins exceed their deflection limit around 28 min. These observations highlight the importance of comprehensive modelling in performance-based fire design. The portal frame model is useful for understanding the overall structural response and identifying potential collapse mechanisms; however, it does not capture the behaviour of purlins, which can influence local failure.

In addition to the industrial hall, a PBD approach was applied to retail occupancy, as well. Given the less severe fire scenarios associated with retail building, the analysis focused on four representative fire scenarios without considering different cases. To achieve a more accurate approximation of the structural response, a reduced torsional stiffness is applied by utilizing a reduction coefficient of 0.1 (*GJ/10*). Warping restraints were not released in the retail building model. The structure resists the entire duration of the fire without collapsing in all four design fire scenarios. Fig. 23 shows the deformed shapes of the structure at the time when the temperature reaches its maximum (30 min). These results indicate that the retail building satisfies the Italian Fire Performance Level 3 (FPC Level 3) in all scenarios, as no structural collapse or critical failure occurs during the design fire exposure.

## 7. Application of fire protection

In the prescriptive design approach, when the structure does not meet the minimum required fire resistance class, passive fire protection material may be used to reduce the effect of fire on the mechanical response and ensure the required exposure time. In this study, a spray-based fire protection material (CAFCO 300 vermiculite spray) was

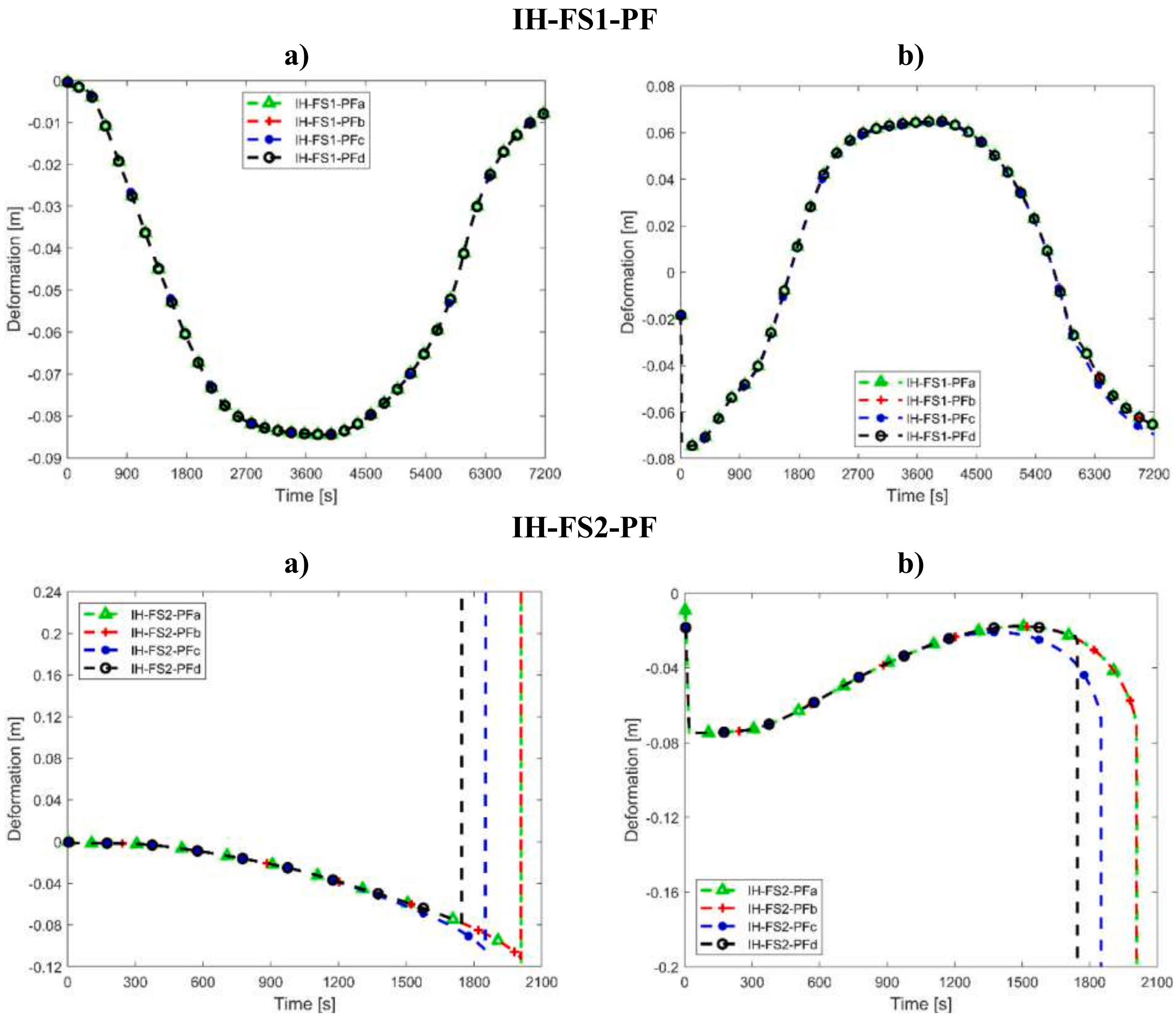


**Fig. 19.** Displacement curves for portal frame models under all cases a) the column top displacement in y direction, b) the rafter midspan displacement in z direction.

selected to apply for structural components. The used fire protection material is characterized by a density of $\rho = 350$ kg/m$^3$, thermal conductivity $\lambda = 0.078$ W/m·K, and specific heat capacity $c = 3300$ J/kg·K. The typical minimum applicable thickness is $d_p = 8$ mm. The numerical model for the protected structure incorporates the temperature-dependent thermal properties of CAFCO300, as determined through experimental studies conducted by Kodur and Shakya [53].

### 7.1. Industrial hall

The required fire resistance rating for the industrial hall is R30. However, prescriptive approach predicts failure time less than 30 min. To enhance the fire performance of the steel structure, passive fire protection was applied exclusively to the rafters and columns.

Table 7 summarizes different configurations for protected industrial hall. In Configuration 1, an 8 mm thick fire protection coating was applied to the IPE550, HE360A, and HE300A sections, while a 10 mm coating was applied to the IPE330A profile. Nevertheless, the structure was unable to withstand the fire for 30 min. Therefore, Configuration 2 applied a 10 mm thick fire protection coating to rafters and columns, and the steel grade of the bracing elements is increased from S235 to S460 to improve lateral stability of the structure. This configuration resulted in the structure collapsing after approximately 31.9 min, thereby meeting the R30 fire resistance requirement. However, the collapse did not occur within the enclosure.

To achieve both the R30 fire resistance requirement and an inward collapse mode, Configuration 3 was implemented. This involved applying an 8 mm thick coating to the IPE550, HE360A, and HE300A sections, and a 10 mm thick coating to the IPE330A and bracing elements. This configuration successfully met the R30 fire resistance requirement, with the structure collapsing after approximately 2562 s (42.7 min).

### 7.2. Retail building

According to the Italian PFC [32], a minimum fire resistance rating of 90 min is required for buildings classified under retail occupancy. Increasing the size of the members and the thickness of fire protection materials are two ways to improve the fire performance of a building beyond prescriptive code-based performance. Table 8 presents the configuration of a protected steel retail building designed to achieve compliance with the R90 fire resistance rate. For the industrial hall, the minimum required thickness of passive fire protection is 8 mm. However, for the retail building, this thickness is increased to 25 mm. The structural response under fire conditions resulted in a failure time of 93.6 min, surpassing the R90 fire resistance requirement.

### 7.3. Cost analysis for fire protection

Under the prescriptive design approach, the structure exposed to the

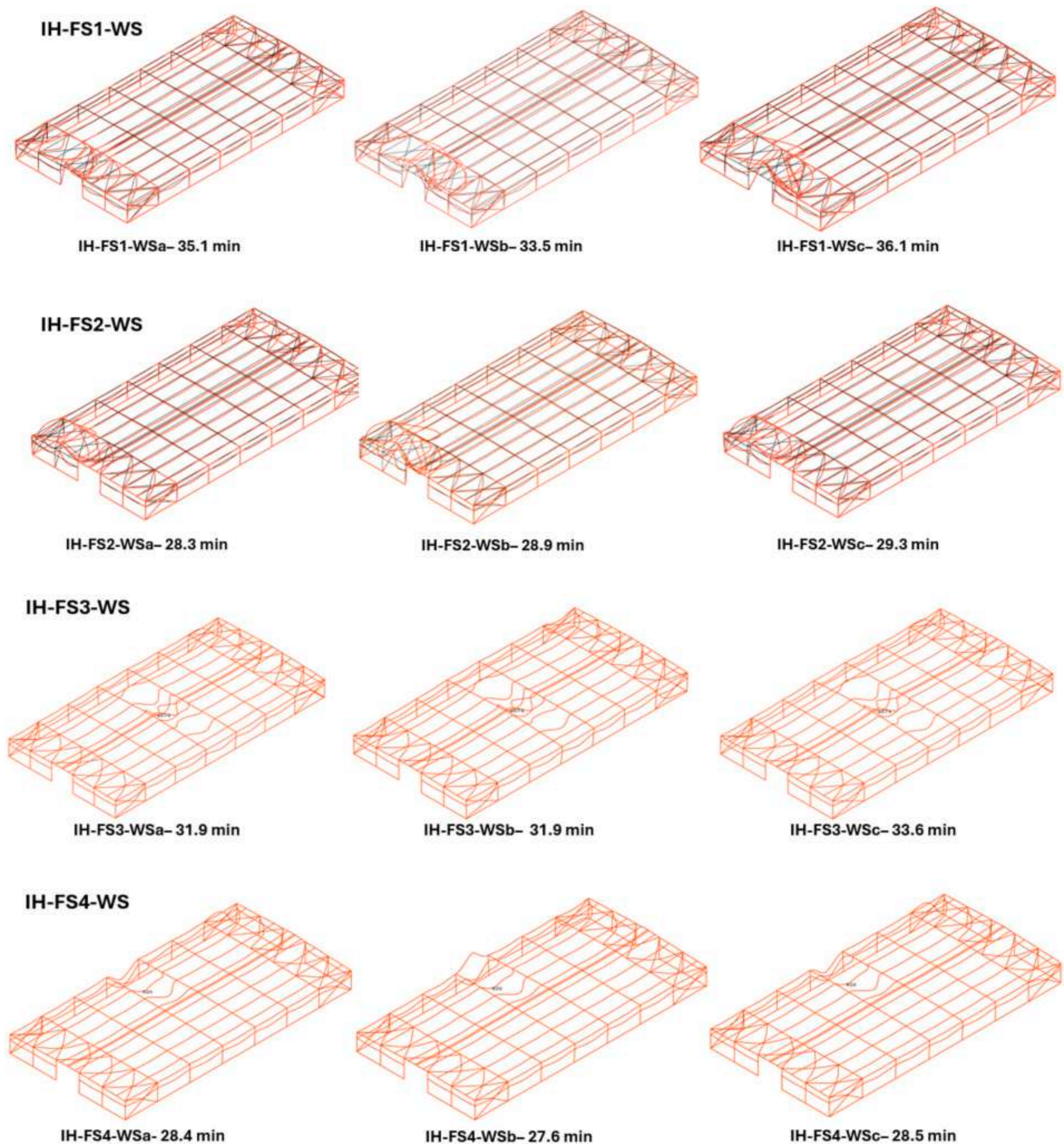


**Fig. 20.** Deflection shapes of industrial halls for each scenario.

standard ISO 834 fire curve fails to meet the required fire resistance classification. Consequently, passive fire protection measures are applied to satisfy the fire design conditions. Table 7 and 8 present the required thicknesses of fire protection materials for each structural component. In contrast, the performance-based design approach employs advanced fire scenarios utilizing localised fire models to assess structural performance. Within this framework, the time for which the load-bearing capacity exceeds twice the Required Safe Egress Time (RSET) across all fire scenarios for both the industrial hall, satisfying the Performance Level II in the context of PBD. For the retail building Performance Level III was satisfied given that the structure survived the entire duration of the design fire scenarios without exhibiting failure. Notably, purlins are not protected under this approach.

This study estimates the total cost of applying fire protection measures which could potentially be avoided through performance-based design approach. The surface areas requiring protection are calculated as 547.8 $m^2$ for the industrial hall and 617.1 $m^2$ for the retail building. CAFCO300 is utilized for passive fire protection. The material cost of CAFCO300 per $m^2$ is approximately 15 euros in Italy. Assuming on-site application by an experienced two-person crew capable of covering 100–150 $m^2$ per day, the application duration is estimated at 5 days for an industrial hall and 6 days for a retail building. Labor costs are estimated at €5 per $m^2$ in the Italian construction sector. The application process requires several pieces of equipment such as scaffolding, spray pumps, air compressors and mixing apparatus. Equipment rental is estimated at €400 per day, aligning with standard rates in the Italian equipment rental market. Transportation and logistics are integral components of the overall cost structure. Considering average distances within Italy and the distribution of construction sites, logistics costs are estimated at €1 per $m^2$. The cumulative cost of fire protection is € 13,503 and €15,358 for industrial hall and retail building, respectively.

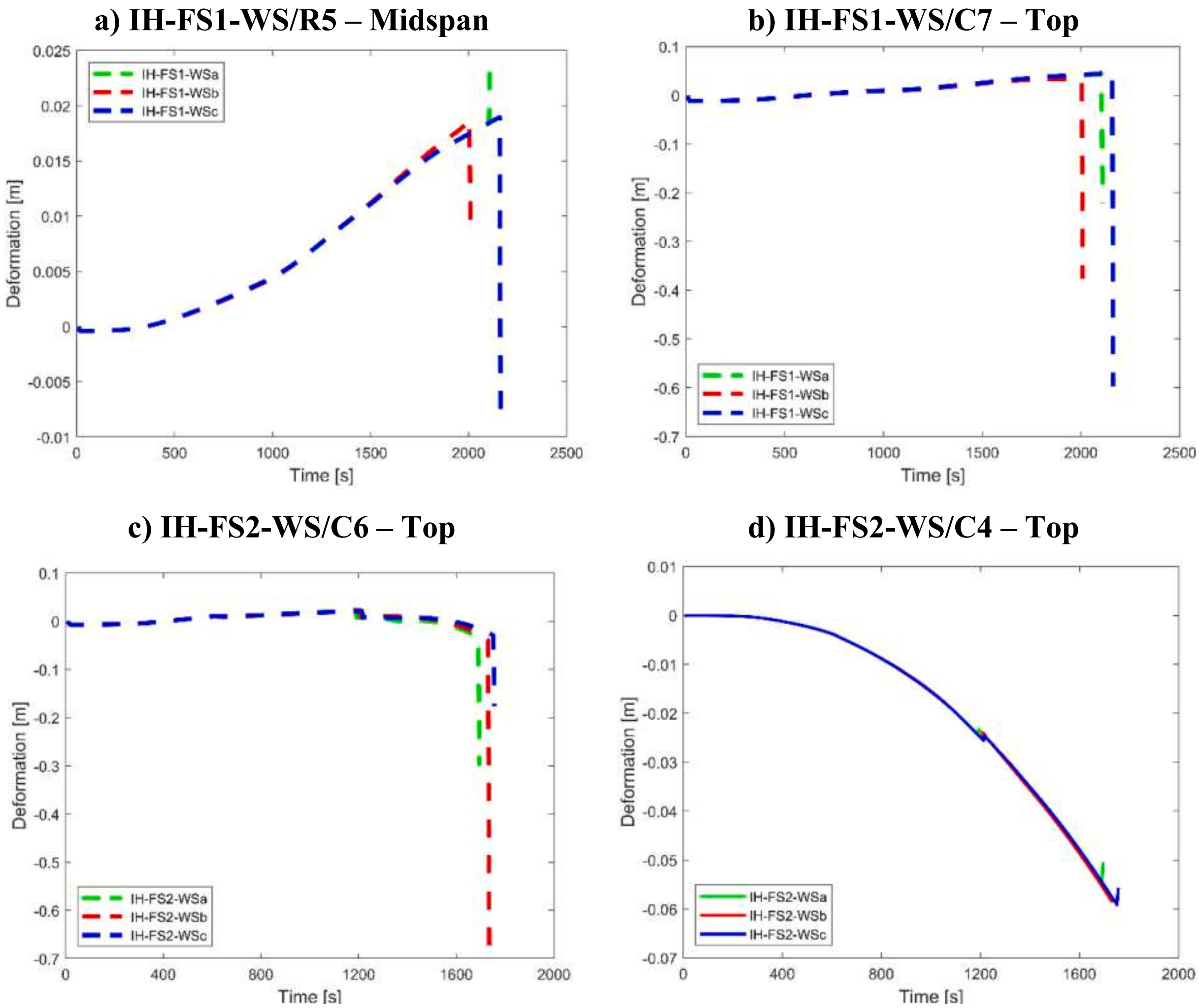


**Fig. 21.** Displacement-time curves for critical components under IH-FS(1–2)-WS.

## 8. Conclusions

This study presented a fire design methodology including prescriptive and performance-based design approach to assess the mechanical response of a single-storey steel structure at elevated temperatures. This paper performed numerical studies on the thermal and mechanical analyses of the single-storey steel structure used as industrial hall and retail buildings under nominal fire curves and localised fires. Several parameters including reduced torsional stiffness, warping release at joints, steel material reversibility above 600 °C, and boundary conditions of the portal frame were investigated to assess their effect on the fire performance of single-storey steel structures. Torsional stiffness and warping significantly influenced the fire response of steel structures. Accurate modelling required adjusting torsional stiffness and warping assumptions according to the considered failure mode and connection type, respectively. The reversibility of steel degradation above 600 °C becomes an important factor in cases of severe fire exposure that include a cooling phase, as the recovery of mechanical properties during cooling can influence the post-fire structural performance. The fire resistance of single-storey portal frame steel structures is strongly influenced by the existence of lateral restraints, which enhance stability and reduce out-of-plane displacements under high-temperature conditions.

The prescriptive approach evaluated the fire performance of the structure exposed to ISO 834 nominal fire curve and compares the failure time with relevant fire resistance classification according to Italian FPC. The PBD approach used localised fire models from new generation of Eurocode to simulate more accurate fire behaviour. Therefore, different fire scenarios for both occupancies were considered varying the position and the intensity of the localised fires in the performance-based design approach. The following results are obtained using the prescriptive approach:

- The unprotected structure collapses after 17.5 min of exposure, indicating a minimum fire resistance rating of R15 and failing to satisfy the requirements for performance levels II and III.
- The fire-protected industrial hall withstands fire exposure for 42.7 min, before collapsing, thereby fulfilling the R30 fire resistance requirement associated with Performance Level II.
- The protected retail building collapses after 93.6 min, ensuring R90 fire resistance and complying with the requirements of Performance Level III.

Using the PBD approach, the following conclusions are drawn:

- Temperature distributions are non-uniform both across the cross-sections of structural components and within the enclosure.
- In Scenario 3, the industrial hall exhibits a minimum predicted failure time of 27.6 min across all scenarios, thus meeting the requirements for Performance Level II without fire protection.
- The retail building maintains structural stability throughout the full duration of all design fire scenarios, satisfying Performance Level III without the use of passive fire protection.

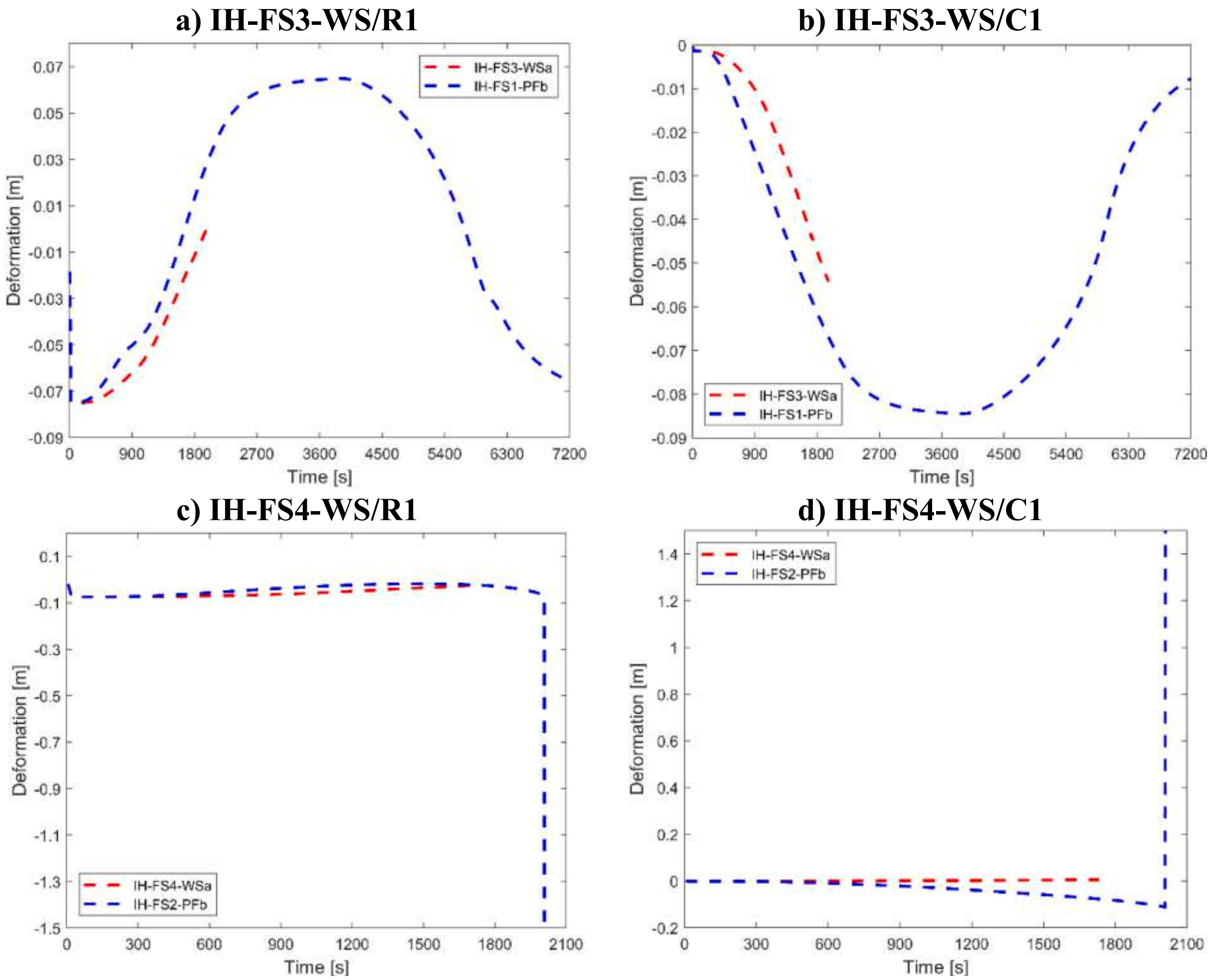


**Fig. 22.** Comparison of deformation curves obtained from the WS and PF model.

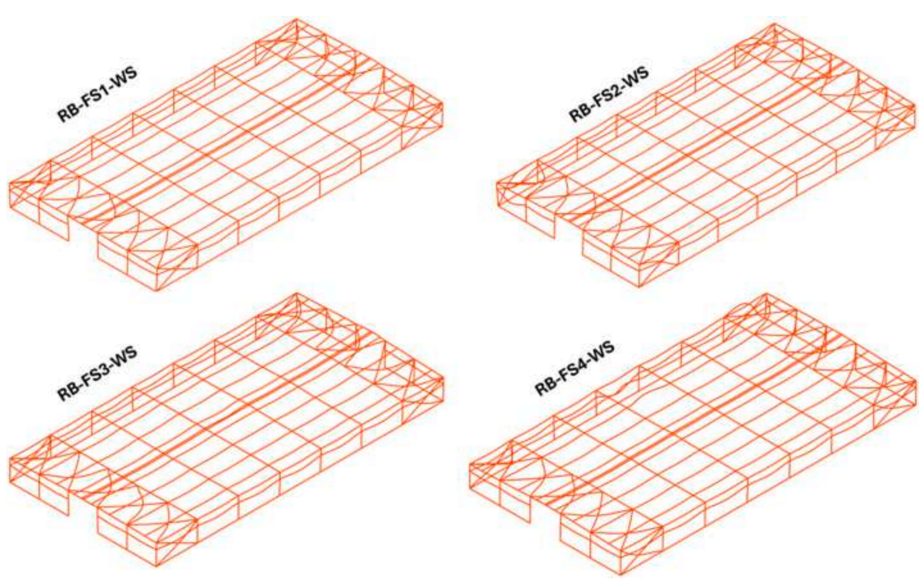


**Fig. 23.** Deflection shapes of retail buildings for each scenario.

- The cost analysis indicates that adopting a performance-based design approach can potentially eliminate the need for passive fire protection measures, resulting in significant cost savings of approximately €13,500 for the industrial hall and €15,400 for the retail building.

In conclusion, the PBFD approach enables a more accurate assessment of a structure's fire performance aligning with the building's specific characteristics and risk profile and can lead to significant cost savings by optimizing or avoiding the use of passive fire protection

**Table 7**
Different configurations for protected industrial halls.

| Description | | | | Failure Mode |
|---|---|---|---|---|
| **Number** | **Member** | **$t_p$ [m]** | **Failure Time [min]** | Sway failure mode |
| | IPE330A | 10 | | |
| | IPE550 | 8 | | |
| | HE300A | 10 | | |
| | HE360A | 8 | | |
| **1** | | | 24.3 < R30 | 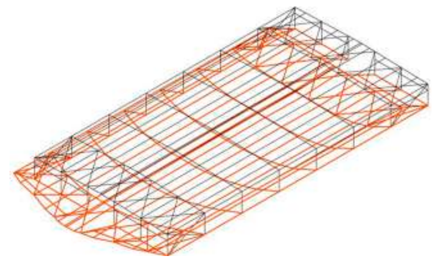 |
| | Braces (S235) | – | | |
| | | | | Sway failure mode |
| | IPE330A | 10 | | |
| | IPE550 | 10 | | |
| | HE300A | 10 | | |
| | HE360A | 10 | | |
| **2** | | | 31.9 > R30 | 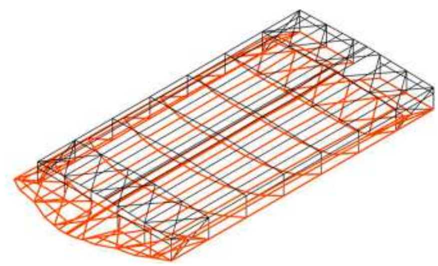 |
| | Braces (S460) | – | | |
| | | | | Inward collapse mode |
| | IPE330A | 10 | | |
| | IPE550 | 8 | | |
| | HE300A | 8 | | |
| | HE360A | 8 | | |
| **3** | | | 42.7 > R30 | 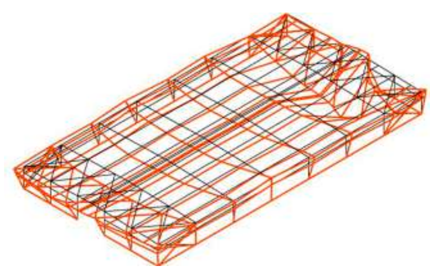 |
| | Braces (S235) | 10 | | |

**Table 8**
Configuration for protected retail building.

| Description | | | | Failure Mode |
|---|---|---|---|---|
| **No** | **Member** | **$t_p$ [mm]** | **Failure Time [min]** | Inward collapse mode |
| | IPE330A | 25 | | |
| | IPE550 | 25 | | |
| | HE300A | 30 | | |
| | HE360A | 25 | | |
| **1** | | | 93.6 > R90 | 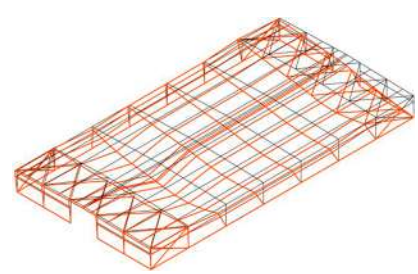 |
| | Braces | 30 | | |

measures. In future work, detailed connection modelling and explicit representation of the roof system should be considered to provide improved restraint to structural components such as purlins. Experimental studies can be used to validate the presented fire design methodology. Furthermore, this design methodology may be extended to multi-storey steel structures.

## CRediT authorship contribution statement

**Batuhan Der:** Writing – review & editing, Writing – original draft, Software, Methodology, Conceptualization. **Oriana Ilnica:** Writing – original draft, Software, Methodology, Conceptualization. **Nicola Tondini:** Writing – review & editing, Writing – original draft, Supervision, Methodology, Investigation, Conceptualization. **Thomas Gernay:** Writing – review & editing, Supervision, Software, Methodology, Conceptualization. **Antoine Glorieux:** Writing – review & editing, Project administration, Investigation, Funding acquisition.

## Declaration of competing interest

The authors declare the following financial interests/personal relationships which may be considered as potential competing interests:

The authors report financial support was provided by ArcelorMittal. Under a license agreement between Gesval S.A. and the Johns Hopkins University, Dr. Gernay and the University are entitled to royalty distributions related to technology SAFIR described in the study discussed in this publication. This arrangement has been reviewed and approved by the Johns Hopkins University in accordance with its conflict of interest policies.

## Acknowledgements

The support received from ArcelorMittal in the context of the project “Automatized choice of fire design of steel structure with new generation of fire models - Knowledge Building Product” is gratefully acknowledged. The third author acknowledges the Italian Ministry of Education, Universities and Research (MUR), in the framework of the project DICAM-EXC (Departments of Excellence 2023-2027, grant L232/2016).

## Data availability

Data will be made available on request.

## References

[1] Y.-C. Wang, T. Lennon, D.B. Moore, The behaviour of single-storey industrial steel frames in fire, Adv. Steel Constr. 5 (3) (2009) 289–302.

[2] P.J. Moss, R.P. Dhakal, M.W. Bong, A.H. Buchanan, Design of steel portal frame buildings for fire safety, J. Constr. Steel Res. 65 (2009) 1216–1224, https://doi.org/10.1016/j.jcsr.2008.09.003.

[3] R. Obiala, O. Vassart, B. Zhao, M.S. Sakji, J. de la Quintana, F. Morente, J.-M. Franssen, J.-B. Lansival, Fire safety of industrial halls — A valorisation project, EUR 24222 EN, Directorate-General for Research, European Commission, Luxembourg (2010), https://doi.org/10.2777/90662.

[4] Z. Huang, Y. Song, Analysis of Industrial Steel Portal Frames in Fire, J. Struct. Fire Eng. 3 (2012) 267–284, https://doi.org/10.1260/2040-2317.3.3.267.

[5] G.-Q. Li, W. Ji, C.-Y. Feng, Y. Wang, G.-B. Lou, Experimental and numerical study on collapse modes of single span steel portal frames under fire, Eng. Struct. 245 (2021) 112968, https://doi.org/10.1016/j.engstruct.2021.112968.

[6] ISO/TR23932–2, Fire safety engineering — General principles —Part 2: Example of a dry-cleaning store, International Organization for Standardization, Geneva, 2020.

[7] G. Spinardi, L. Bisby, J. Torero, A review of sociological issues in fire safety regulation, Fire Technol. 53 (2017) 1011–1037, https://doi.org/10.1007/s10694-016-0615-1.

[8] N.E. Khorasani, P. Gardoni, M.E.M. Garlock, Probabilistic fire analysis: Material models and evaluation of steel structural members, J. Struct. Eng. 141 (2015) 04015050, https://doi.org/10.1061/(ASCE)ST.1943-541X.0001285.

[9] T. Gernay, N.E. Elhami-Khorasani, Recommendations for performance-based fire design of composite steel buildings using computational analysis, J. Constr. Steel Res. 166 (2020) 105906, https://doi.org/10.1016/j.jcsr.2019.105906.

[10] J. Randaxhe, N. Popa, N. Tondini, Probabilistic fire demand model for steel pipe-racks exposed to localised fires, Eng. Struct. 226 (2021) 111310, https://doi.org/10.1016/j.engstruct.2020.111310.

[11] T. Jokinen, R. Ranua, M. Kauriala, M. Salminen, Holistic performance-based fire design of steel structures—Case study: Sports hall, Fire Technol. 60 (2024) 2785–2814, https://doi.org/10.1007/s10694-023-01461-7.

[12] S. Mostofi, A. Baltaci, Y.E. Akbulut, F.Y. Okur, A.C. Altunişik, Performance-based fire assessment of a fully automated multi-storey steel parking structure: A computational approach, Case Stud. Therm. Eng. 48 (2024) 104618, https://doi.org/10.1016/j.csite.2024.104618.

[13] T. Gernay, Performance-based design for structures in fire: Advances, challenges, and perspectives, Fire Saf. J. 142 (2024) 104036, https://doi.org/10.1016/j.firesaf.2023.104036.

[14] X. Yan, T. Gernay, Numerical modeling of localised fire exposures on structures using FDS-FEM and simple models, Eng. Struct. 246 (2021) 112997, https://doi.org/10.1016/j.engstruct.2021.112997.

[15] A.A. Khan, A. Usmani, J.L. Torero, Evolution of fire models for estimating structural fire-resistance, Fire Saf. J. 124 (2021) 103367, https://doi.org/10.1016/j.firesaf.2021.103367.

[16] D. Lange, J. Sjöström, Mechanical response of a partially restrained column exposed to localised fires, Fire Saf. J. 67 (2014) 82–95, https://doi.org/10.1016/j.firesaf.2014.05.013.

[17] C. Zhang, Z. Zhang, G.Q. Li, Simple vs. sophisticated fire models to predict performance of SHS column in localised fire, J. Constr. Steel Res. 120 (2016) 62–69, https://doi.org/10.1016/j.jcsr.2015.12.019.

[18] N. Tondini, J.-M. Franssen, Analysis of experimental hydrocarbon localised fires with and without engulfed steel members, Fire Saf. J. 92 (2017) 9–22, https://doi.org/10.1016/j.firesaf.2017.05.011.

[19] T. Chu, L. Jiang, G. Zhu, A. Usmani, Fire impact on vertical components subjected to a localised fire estimated using a line source model, Fire Technol. 59 (2023) 2299–2331, https://doi.org/10.1007/s10694-023-01429-0.

[20] L. Possidente, C. Couto, N. Tondini, P.V. Real, Review of design approaches for steel columns subjected to localised fires: Insights from the 2nd generation Eurocode model, Eng. Struct. 315 (2024) 118424, https://doi.org/10.1016/j.engstruct.2023.118424.

[21] C. Zhang, G.Q. Li, A. Usmani, Simulating the behaviour of restrained steel beams to flame impingement from localised fires, J. Constr. Steel Res. 83 (2013) 156–165, https://doi.org/10.1016/j.jcsr.2013.02.001.

[22] C. Zhang, J.L. Gross, T.P. McAllister, Lateral torsional buckling of steel W-beams subjected to localised fires, J. Constr. Steel Res. 90 (2013) 163–173, https://doi.org/10.1016/j.jcsr.2013.06.004.

[23] X.T. Nguyen, J.S. Park, Nonlinear buckling strength of steel H-beam under localised fire and pure bending, KSCE J. Civ. Eng. 25 (2021) 561–573, https://doi.org/10.1007/s12205-020-0291-z.

[24] S. Suman, A. Samanta, Behaviour of unrestrained hot-rolled steel I-beams exposed to localised fire: An experimental study, Eng. Struct. 296 (2023) 116953, https://doi.org/10.1016/j.engstruct.2023.116953.

[25] Y. Xia, M. Charlier, T. Gernay, Thermal response of steel framing members in open car park fires, Front. Struct, Civ. Eng. 16 (2022) 1071–1088, https://doi.org/10.1007/s11709-022-0879-0.

[26] J. Jiang, C. Wang, G. Lou, G.-Q. Li, Quantitative evaluation of progressive collapse process of steel portal frames in fire, J. Constr. Steel Res. 150 (2018) 11–22, https://doi.org/10.1016/j.jcsr.2018.09.001.

[27] W. Ji, G.Q. Li, G.B. Lou, Y. Wang, S. Zhu, Early-warning methods for fire-induced collapse of single span steel portal frames, J. Constr. Steel Res. 190 (2022) 107154, https://doi.org/10.1016/j.jcsr.2022.107154.

[28] H.H. Qi, G.-B. Lou, Y. Pang, G.-Q. Li, Early-warning approach for fire-induced collapse of steel portal frame based on overall deformation, J. Build. Eng. 101 (2025) 111835, https://doi.org/10.1016/j.jobe.2025.111835.

[29] CEN, Eurocode 1: Actions on structures – Part 1–2: General actions – Actions on structures exposed to fire, EN 1991–1-2, European Committee for Standardization, Brussels, 2021.

[30] O. Vassart, F. Hanus, R. Obiala, M. Brasseur, J.-M. Franssen, A. Scifo, B. Zhao, C. Thauvoye, A. Nadjai, S. Han, R. Zaharia, D. Pintea, Temperature assessment of a vertical steel member subjected to localised fire (LOCAFI), in: EUR 28577 EN, Directorate-General for Research and Innovation, European Commission, Luxembourg, 2017, https://doi.org/10.2777/67601.

[31] N. Tondini, C. Thauvoye, F. Hanus, O. Vassart, Development of an analytical model to predict the radiative heat flux to a vertical element due to a localised fire, Fire Saf. J. 105 (2019) 227–243, https://doi.org/10.1016/j.firesaf.2019.03.001.en.

[32] Ministero dell'Interno, Italian Fire Prevention Code (English translation). Decree of the President of the Republic, 1 Aug. 2011, no. 151. Regulations for simplified application of the discipline procedures relating to fire prevention activities, 2015. Retrieved from, https://cfpa-e.eu/app/uploads/2020/09/Codice-in-inglese.pdf.

[33] F. Bontempi, C. Crosti, E. Nigro, A. Ferraro, S. Pustorino, P. Princi, L. Ponticelli, C. Mastrogiuseppe, Fire design of steel structures in industrial halls — Thermo-fluid dynamic modelling of fire scenarios, Fondazione Promozione Acciaio, Milan, 2015.

[34] J.M. Franssen, T. Gernay, Modeling structures in fire with SAFIR®: theoretical background and capabilities, J. Struct. Fire Eng. 8 (2017) 300–323, https://doi.org/10.1108/JSFE-07-2017-0023.

[35] J-F. Cadorin, J.-M. Franssen, A tool to design steel elements submitted to compartment fires—OZone V2. Part 1: pre- and post-flashover compartment fire model, J. Struct. Fire Eng. 2 (2011) 29–44. doi: https://doi.org/10.1108/2040 2361111108304.

[36] M.J. Hurley (Ed.), SFPE Handbook of Fire Protection Engineering, 5th edition, Springer, New York, 2016.

[37] ISO, Fire-safety engineering — Technical information on methods for evaluating behaviour and movement of people, ISO/TR 16738,, International Organization for Standardization, Geneva, Switzerland, 2009.

[38] BSI, Application of fire safety engineering principles to the design of buildings – Part 6: Human factors – Life safety strategies – Occupant evacuation, behaviour and condition (Sub-system 6), PD 7974–6:2019, British Standards Institution, London, UK, 2019.

[39] M.M.S. Dwaikat, V.K.R. Kodur, S.E. Quiel, M.E.M. Garlock, Experimental behaviour of steel beam–columns subjected to fire-induced thermal gradients, Journal of Constructional Steel Research 67 (1) (2011) 30–38, https://doi.org/10.1016/j.jcsr.2010.07.007.

[40] N. Tondini, A. Morbioli, O. Vassart, S. Lechêne, J.-M. Franssen, An integrated modelling strategy between a CFD and an FE software: Methodology and application to compartment fires, J. Struct. Fire Eng. 7 (2016) 217–233, https://doi.org/10.1108/JSFE-09-2016-015.

[41] C. Maraveas, T. Gernay, J.-M. Franssen, An equivalent stress method to account for local buckling in beam finite elements subjected to fire, J. Struct. Fire Eng. 10 (2019) 340–353, https://doi.org/10.1108/JSFE-09-2018-0020.

[42] S. Ni, X. Yan, M.S. Hoehler, T. Gernay, Numerical modeling of the post-fire performance of strap-braced cold-formed steel shear walls, Thin-Walled Struct. 171 (2022) 108733, https://doi.org/10.1016/j.tws.2021.108733.

[43] CEN, Eurocode 3: Design of steel structures – Part 1–2: General rules – Structural fire design, EN 1993-1-2,, European Committee for Standardization, Brussels, 2023.

[44] B. Der, S. Raszková, F. Wald, G. Bihina, C. Gaigl, V. Rus, M. Malaska, Emissivity of hot-dip galvanized surfaces in future development of EN 1993-1-2, J. Struct. Fire Eng. 13 (4) (2022) 535–557, https://doi.org/10.1108/JSFE-11-2021-0070.

[45] P.D. Simão, J.P.C. Rodrigues, Consistent thermodynamics analysis of restrained steel columns in fire – Part 1: Theoretical developments for general application, Eng. Struct. 295 (2025) 120591, https://doi.org/10.1016/j.engstruct.2025.120591.

[46] P.D. Simão, J.P.C. Rodrigues, Consistent thermodynamics analysis of restrained steel columns in fire – Part 2: Application to the voxels-based Rayleigh–Ritz method, Eng. Struct. 295 (2025) 120590, https://doi.org/10.1016/j.engstruct.2025.120590.

[47] L. Possidente, N. Tondini, J.M. Battini, 3D beam element for the analysis of torsional problems of steel structures in fire, J. Struct. Eng. 146 (2020) 04020125, https://doi.org/10.1061/(ASCE)ST.1943-541X.0002630.

[48] M. Kucukler, Stainless steel I-section beams at elevated temperatures: Lateral–torsional buckling behaviour and design, Thin–Walled Struct. 208 (2025) 112720, https://doi.org/10.1016/j.tws.2021.112720.

[49] J.-M. Franssen, B. Cowez, T. Gernay, Effective stress method to be used in beam finite elements to take local instabilities into account, Fire Saf. Sci. 11 (2014) 544–557, https://doi.org/10.3801/IAFSS.FSS.11-544.

[50] Ministero delle Infrastrutture e dei Trasporti, Technical Standards for Construction (NTC 2018). Ministerial Decree of 17 January 2018. Published in the Official Gazette of the Italian Republic, General Series No. 42, 20 February 2018, 2018.

[51] CEN, EN 1990:2002/A1 Eurocode – Basis of Structural Design, European Committee for Standardization, Brussels, 2005.

[52] CEN, Eurocode 3: Design of steel structures – Part 1–1: General rules and rules for buildings, in: European Committee for Standardization, EN 1993-1-1:2022, Brussels, 2022.

[53] V.K.R. Kodur, A.M. Shakya, Effect of temperature on thermal properties of spray-applied fire resistive materials, Fire Saf. J. 61 (2013) 314–323, https://doi.org/10.1016/j.firesaf.2013.09.011.